University of Houston

Department of Electrical and Computer Engineering

Enhancing Frequency Stability of Low-Inertia Grids with Novel Security Constrained Unit Commitment Approaches

Mingjian Tuo

June 19, 2023

Committee Members: Xingpeng Li, Ph. D. (Chair)
Kaushik Rajashekara, Ph. D.
Zhu Han, Ph. D.
Lei Fan, Ph. D.
David R. Jackson, Ph. D.

UH RPG Lab

Overview

1. Introductions
2. Physics-based Inertia Estimation
3. Machine Learning Assisted Inertia Estimation
4. Physics-based Locational RoCoF-constrained Unit Commitment
5. Deep Learning based RCUC
6. Active Linearized Sparse Neural Network based FCUC
7. Conclusion and Future Work

The Elements of Power System

A power system is an electrical network of interconnected elements that are used to generate, transmit, and consume electric power. It contains various types of elements:

- Generators
- Loads
- Transmission lines
- Transformers
- Phase shifters
- Circuit breakers
- Shunts
- HVDC
- … …




Generation

Transmission & Distribution




Consumption

Energy Balance

Ideal Scenario:
The total power generated in a power system should match the total power consumed by the loads.

Real Situation:
- fluctuations in load demand,
- power losses in transmission and distribution
- uncertainties in renewable energy generation

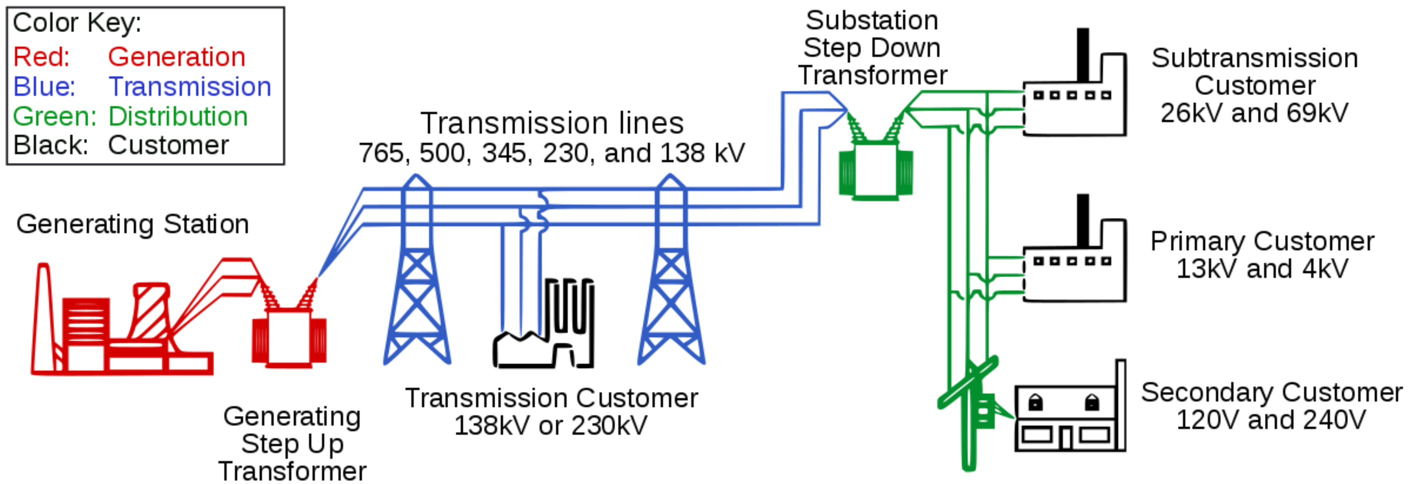

https://figshare.com/articles/online_resource/ECE6379_PSOM_zip/17161805

Power System Management

Power system management problems can be divided into a few groups based on time-scale:

- 5-40 years: power system expansion planning
- 1-3 years: maintenance scheduling for large equipment, long-term bilateral contracts, generation capacity commitment
- 1 day - 1 week: maintenance scheduling for medium and small equipment; power system operational planning
- 1 day: day-ahead scheduling (through SCUC)
- 5-30 minutes: contingency analysis, look-ahead dispatching
- < 1 minute: system control, frequency regulation, stability

https://figshare.com/articles/online_resource/ECE6379_PSOM_zip/17161805

Power System Frequency

- Generators rotate in synchronism to produce electric power.
- Frequency: the speed of rotation of synchronized generators.
  - measured in cycles per second, or Hertz (Hz).
- Normal situations: generation and load are balanced
- Rotate speed: 60 cycles per second.
- The nominal system frequency : 60 Hz.

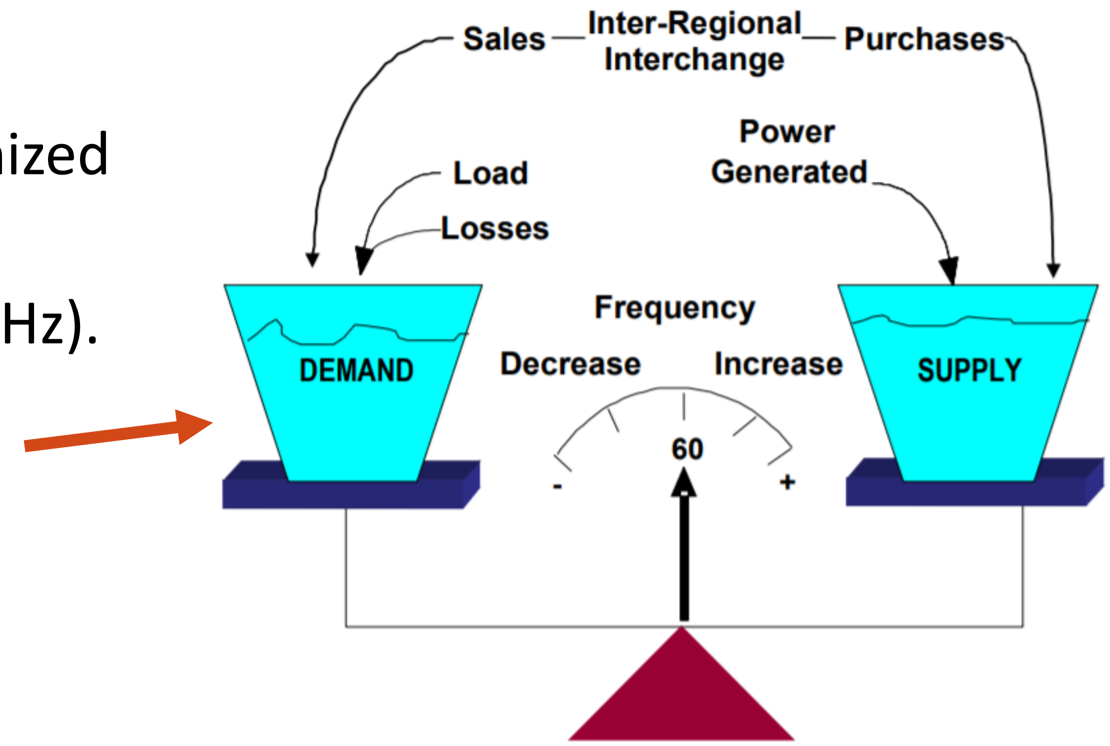

[Reference] NERC, “Balancing and Frequency Control”, a technical document prepared by the NERC Resources Subcommittee, January 26, 2011.

Problem Setup

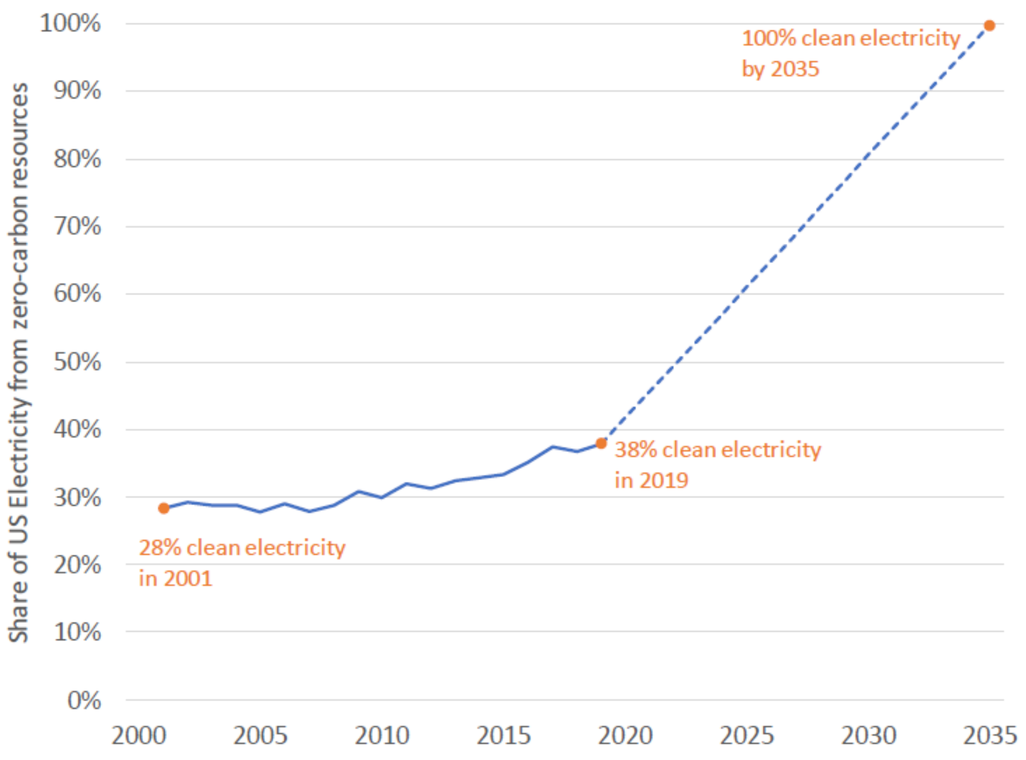

Figure. Percentage of U.S. electricity generation from clean energy resources from 2001 to 2035

- 1) Units with governor providing primary frequency response are replaced by non-dispatchable units
- 2) non-dispatchable, asynchronous (converter-based) units present low to zero contribution to the total inertia of the system.

- Estimation of system inertia provides more information for system operation.
- Impose extra constraints in the conventional SCUC model to secure frequency stability.

[Reference] D. Lew, J. Bakke, A. Bloom, P. Brown, J. Caspary, C. Clack, N. Miller, A. Orths, A. Silverstein, J. Simonelli, and R. Zavadil, ``Transmission planning for 100% clean electricity: Enabling clean, affordable, and reliable electricity,'' IEEE Power Energy Mag., vol. 19, no. 6, pp. 5666, Nov. 2021.

Contributions and Organization

Physics-based Inertia Estimation	Machine Learning Assisted Inertia Estimation	Physics-based RoCoF Constrained Unit Commitment	Deep Learning based RCUC	Active Linearized Sparse Neural Network Based FCUC	Conclusion and Future Work
•Estimates the dynamic system inertia distribution •Determines the center of inertia (COI) area •Dynamic inertia estimation	•System Perturbation using Probing Signal •LRCN based inertia estimation •GCN based inertia estimation	•Location based RoCoF constrained SCUC model •Multiple-measurement-window method •Virtual inertia-based SCUC models.	•Model based data generation on PSS/E •Incorporate non-linear DNN/CNN model into RCUC formulation	•Deep learning-based frequency metrics tracking •Dynamic pruning in DNN-based FCUC model •Active ReLU linearization approximation	

Power System Inertia

Inertia (MWs): kinetic energy E_i stored in the rotating shaft of a synchronous generator

$$E_i = \frac{1}{2} J_i \, \omega_n^2$$

Inertia constant(s): ratio of kinetic energy of a rotor of a synchronous machine to the rating of a machine.

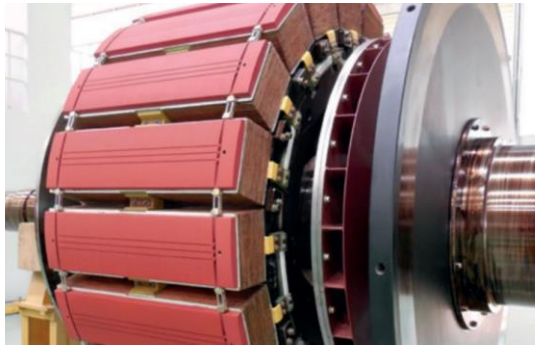

$$H_i = \frac{E_i}{S_i} = \frac{\frac{1}{2} J_i \, \omega_n^2}{S_i}$$

Inertia in power systems refers to the energy stored in large rotating synchronized generators and some industrial motors.

$$E_{sys} = \sum_{i=1}^{N} \frac{1}{2} J_i {\omega_i}^2 = \sum_{i=1}^{N} H_i S_{B_i}$$

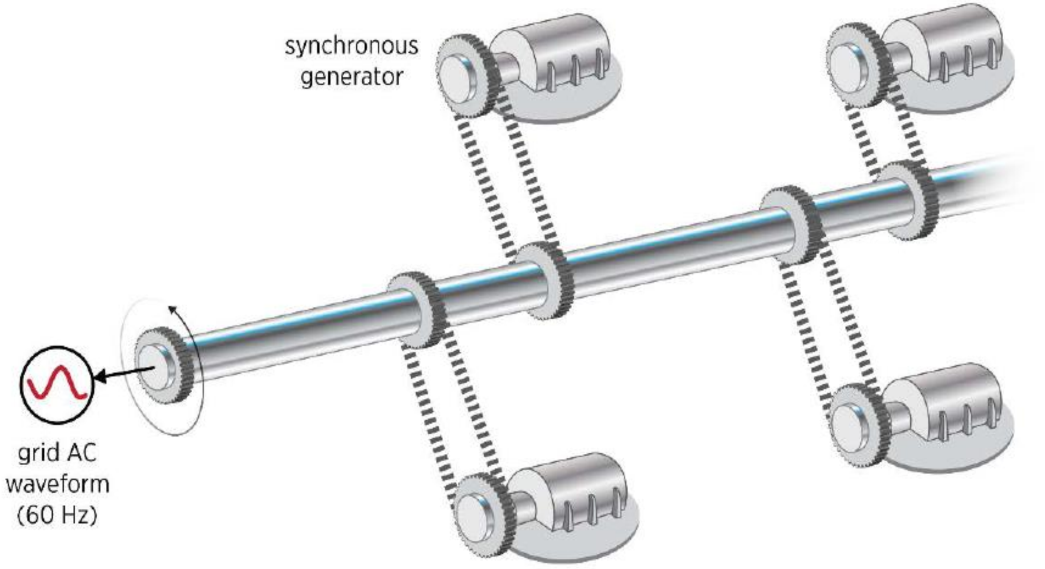

Figure. Synchronized generators within a system

[Reference] P. Denholm, T. Mai, R. W. Kenyon, B. Kroposki, and M. O'Malley. Inertia and the Power Grid: A Guide Without the Spin. Tech. rep. National Renewable Energy Laboratory, 2020

Traditional Inertia Estimation

System operators measure the frequency at some relevant pilot bus of the system.

$$E_{sys} = \frac{-\Delta P}{2\frac{d\omega}{dt}} \cdot \omega_0$$

Factors impact inertia estimation:

- 1) disturbance level ΔP
- 2) location of measurement bus relative to in-feed disturbance
- 3) method of RoCoF calculation $\frac{d\omega}{dt}$

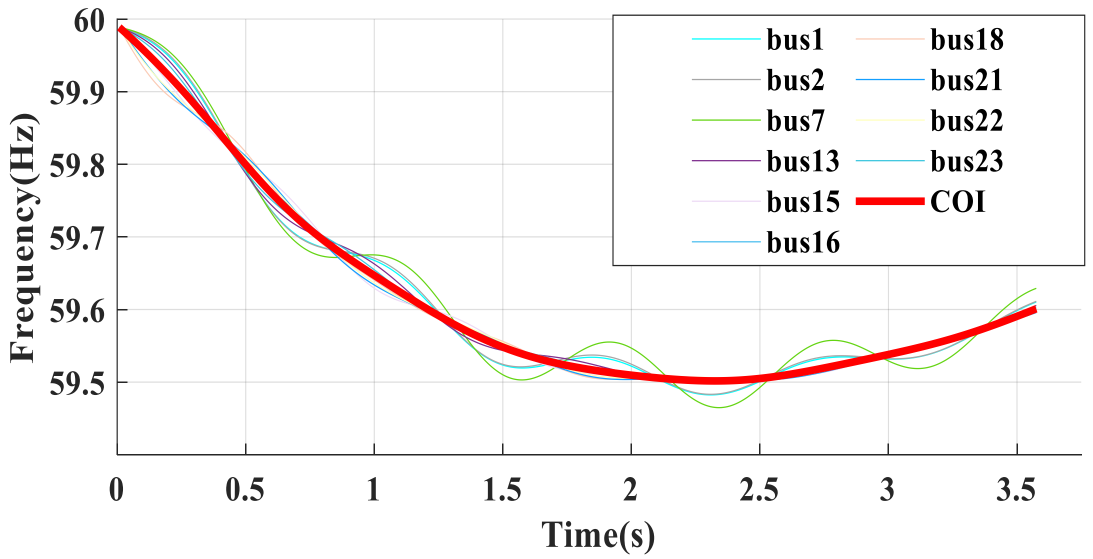

Figure. Frequency dynamics on generator buses in IEEE-24 bus system

The pilot bus (representing COI) cannot be able to capture the entire characteristics.

Inertia Distribution Index

- Following one disturbance, the electrical distance from an estimated bus k to COI then be calculated below:

$$d_k = \int_{t_0+t_d}^{T+t_0+t_d} (f_k(\tau) - f_{COI}(\tau))^2 d\tau$$

- Inertia distribution index (IDI):

$$IDI_k = \frac{d_k}{\max\limits_{k \in \{1,..,n\}} d_k}$$

$$k_{COI} = argmin(IDI_k)$$

The set of COI area buses over period T_{win} is then defined as:

$$S_{COI}^{T_{win}} = \left\{k^t\colon\, dist\left(f^t{}_k, f^t{}_{k_{COI}}\right) \le \delta, t \in T_{win}\right\}$$

where $f^t{}_{k_{COI}}$ is the frequency measurements on COI bus k_{COI}

Dynamic Inertia Estimation

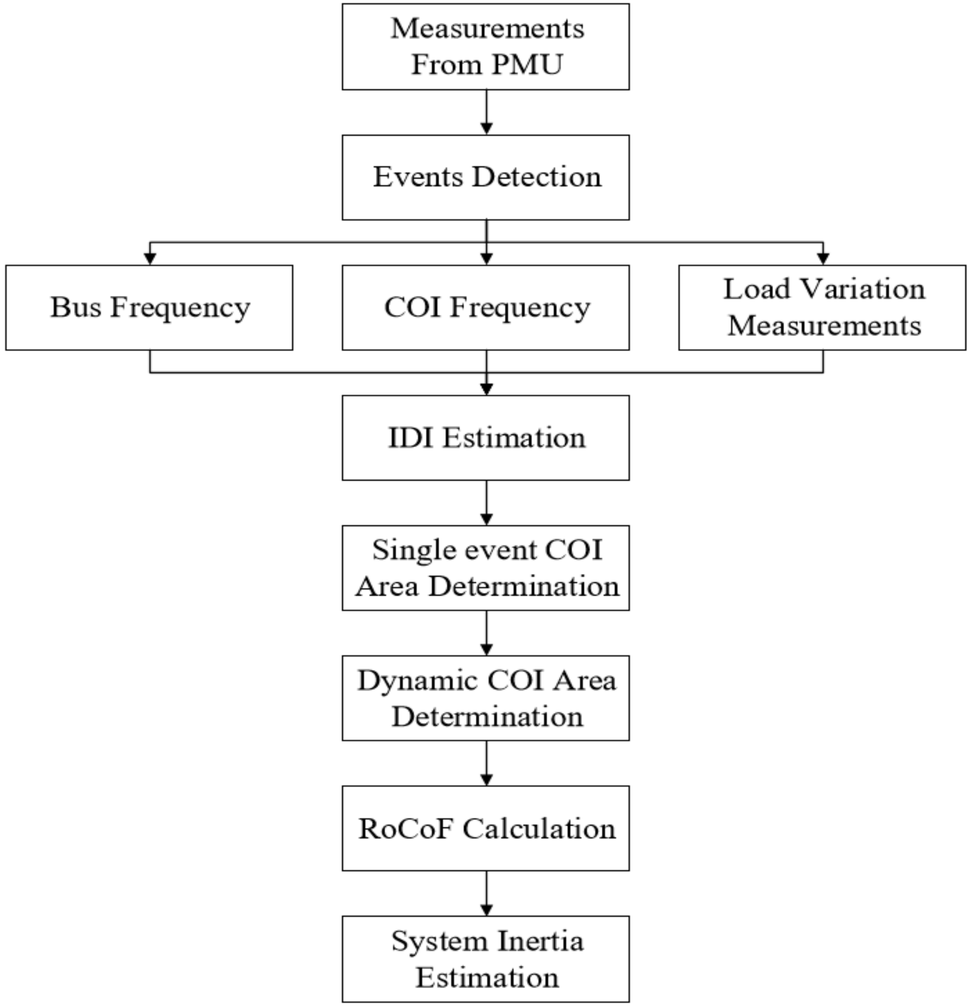

Fig.1 System inertia estimation process on events.

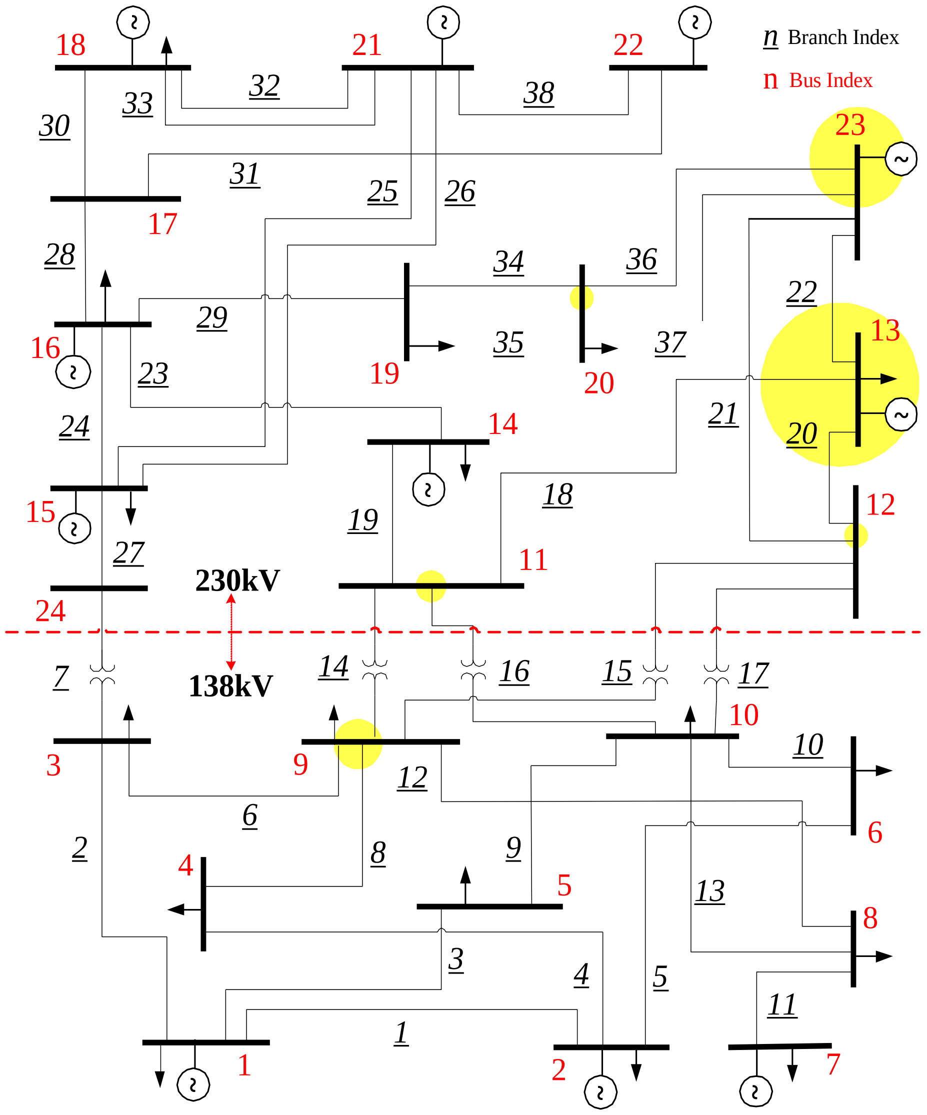

Fig.2 Center of inertia area estimation in IEEE 24-bus system.

Dynamic Inertia Estimation

Following a disturbance event, the pilot bus is selected as the initial point in the COI area cluster set.

$$k_{COI}^{T_{win}} = \arg \max_{k \in \{1,..,n\}} C_k$$

Where C_k is the count of bus k identified as a bus of the COI area.

$$\frac{df_{est}}{dt} = \frac{C_k}{C_p + C_k} \cdot \frac{df_k}{dt} + \frac{C_p}{C_p + C_k} \cdot \frac{df_p}{dt}, \qquad p, k \in S_{COI}^{T_{win}}$$

Table Results of Inertia Estimation

H_{real} **(MWs)**	H_{COI} **(MWs)**	$\%H_{dif}^{COI}$	H_{prop} **(MWs)**	$\%H_{dif}^{prop}$
31525.0	30044.6	-4.70%	30600.9	-2.93%

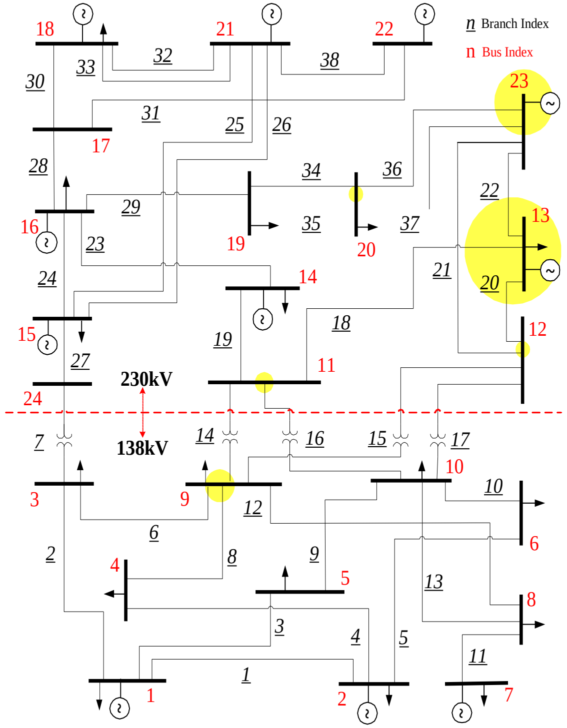

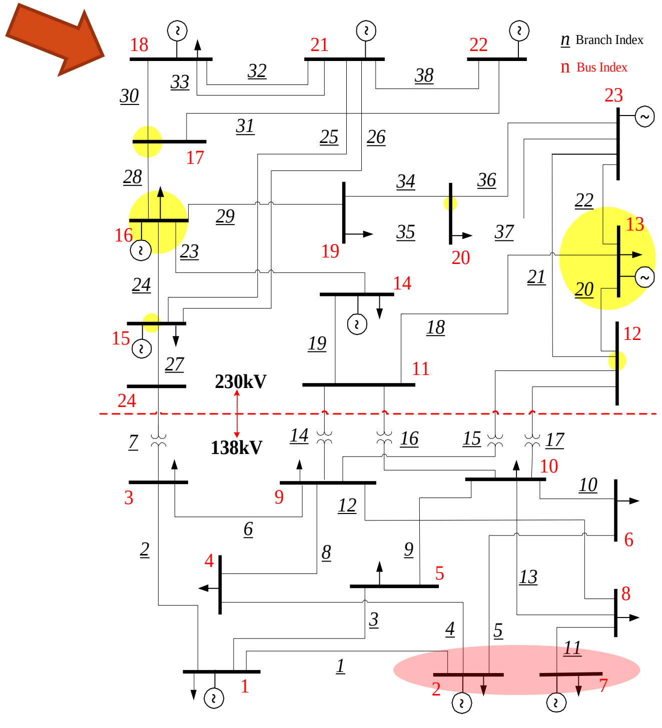

Fig.1 COI area of case with 20% RES penetration level.

Summary

- Dynamic inertia estimation method based on COI area is proposed.
- Sensitivity test is then conducted to determine the optimal time length of integration period.
- The proposed inertia estimation method is more robust and accurate for estimating system inertia distribution

1. **Mingjian Tuo** and Xingpeng Li, “Dynamic Estimation of Power System Inertia Distribution Using Synchrophasor Measurements”, *2020 52nd North American Power Symposium (NAPS)*, Apr. 2021, pp. 1-6, doi: 10.1109/NAPS50074.2021.9449713.

1. Introductions
2. Physics-based Inertia Estimation
3. Machine Learning Assisted Inertia Estimation
4. Physics-based Locational RoCoF-constrained Unit Commitment
5. Deep Learning based RCUC
6. Active Linearized Sparse Neural Network based FCUC
7. Conclusion and Future Work

System Dynamics

Power mismatch event process:

- Frequency drop from nominal value
- Deviation measurement is fed into closed control droop
- Turbine-governor counteracts the power mismatch

Measurements:

- Frequency
- Analogue voltage
- Current wave

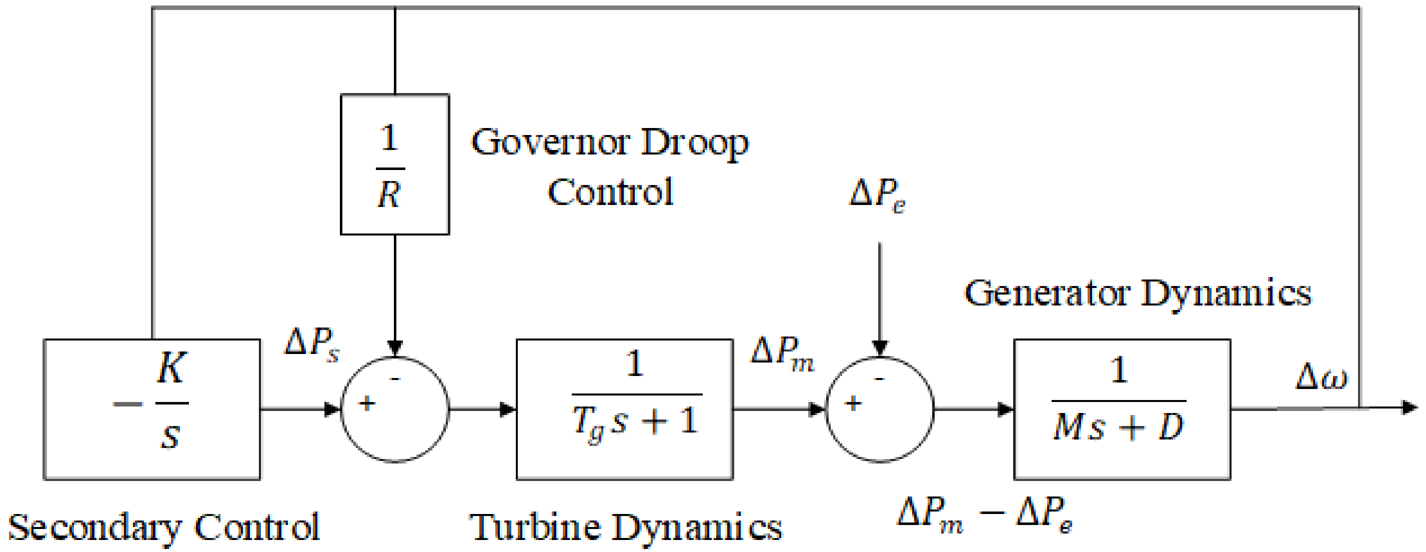

Figure. Generator transfer function model.

Wide Area Monitoring System

Conventional Supervisory Control and Data Acquisition (SCADA) systems

- Steady information system
- Resolution between 1 and 10 s.

Wide Area Monitoring System (WAMS)

- Phasor Measurement Unit (PMU)
- Time-synchronized information.
- Reporting rates: 10-240 samples per second.

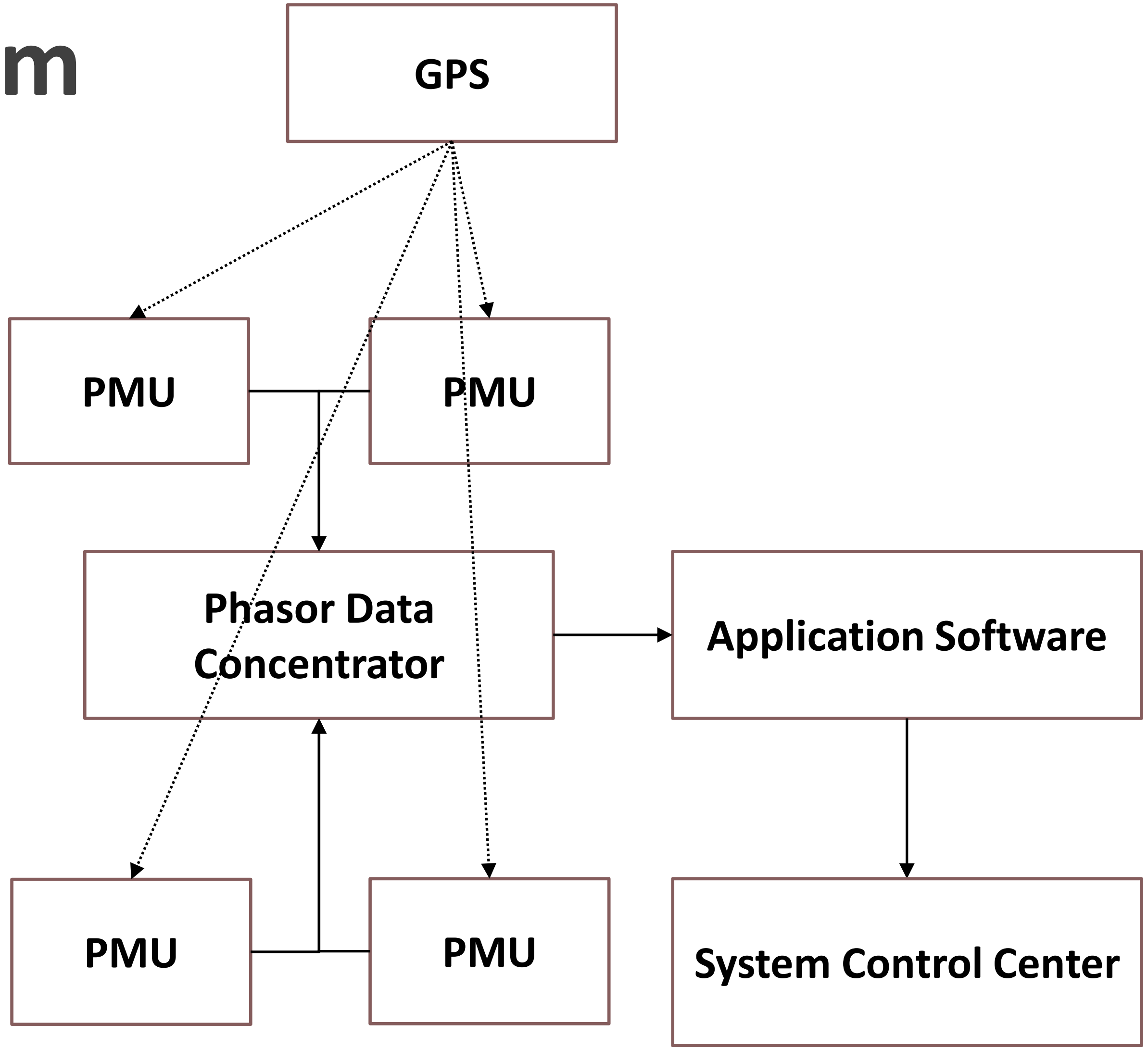

Figure. Example of WAMS.

Probing Signal Method

Low level probing signal method has been conventionally used for generator dynamic studies

(Excitation signals with 100 different values of P_E from 0.001 p.u. to 0.01 p.u. with an increment 0.001 p.u. were used)

Measurements:

- Frequency deviations
- RoCoF measurements
- Voltage dynamics

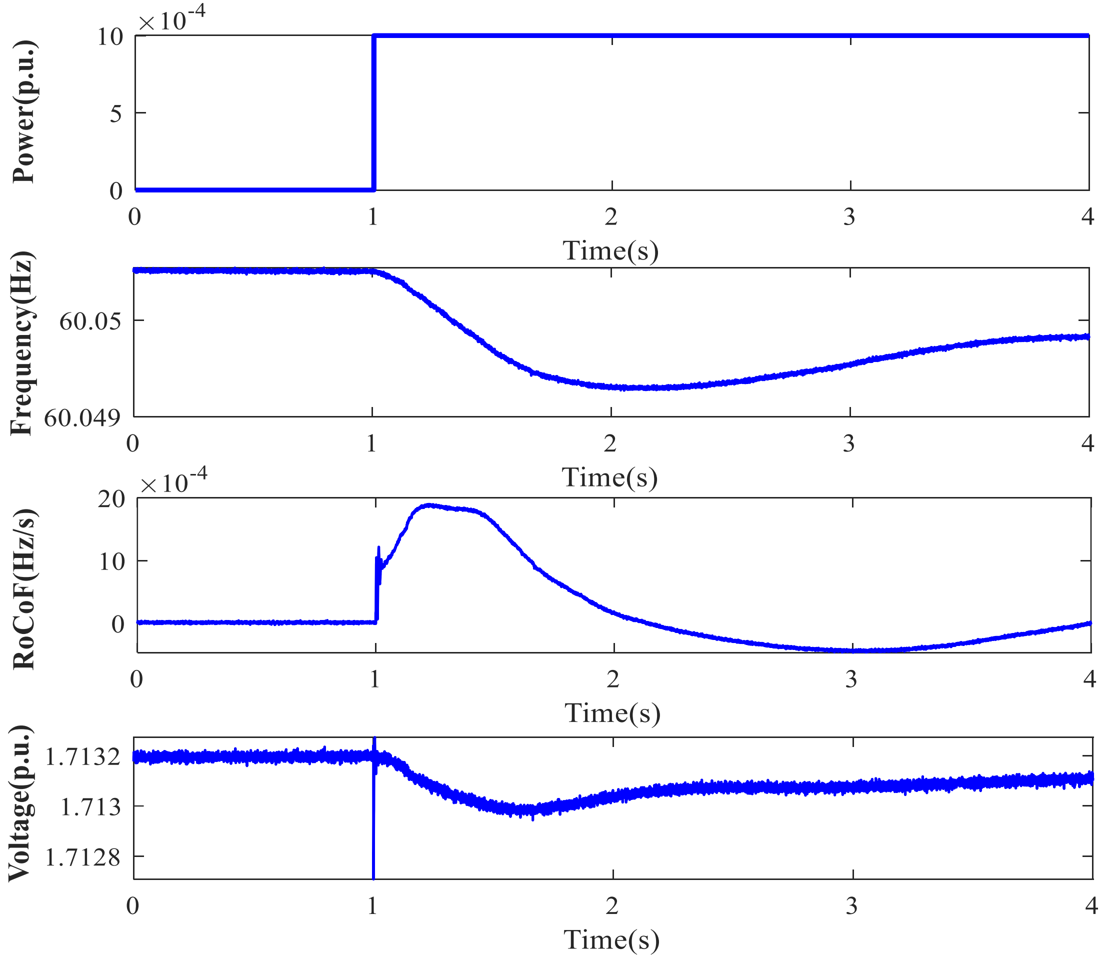

Figure. A sample of probing signal, ambient measurements for P_E=0.001 p.u.

Inertia Estimation Using LRCN

- Long-term recurrent convolutional network (LRCN) is used to process temporal input data and identify spatial features of ambient wide measurements.
- The neural network based systemwide inertia estimator $\hat{h}$ can be expressed as

$$\hat{I} = \hat{h}(x, W, b)$$

- where x is the input feature vector, and W and b denote the parameters of a well-trained LRCN model.
- Forward propagation equation (LRCN):

$$h_t = (1 - z_t) * h_{t-1} + z_t * h_t$$

$$z_t = \sigma(W_f [h_{t-1}, x_t] + b_f)$$

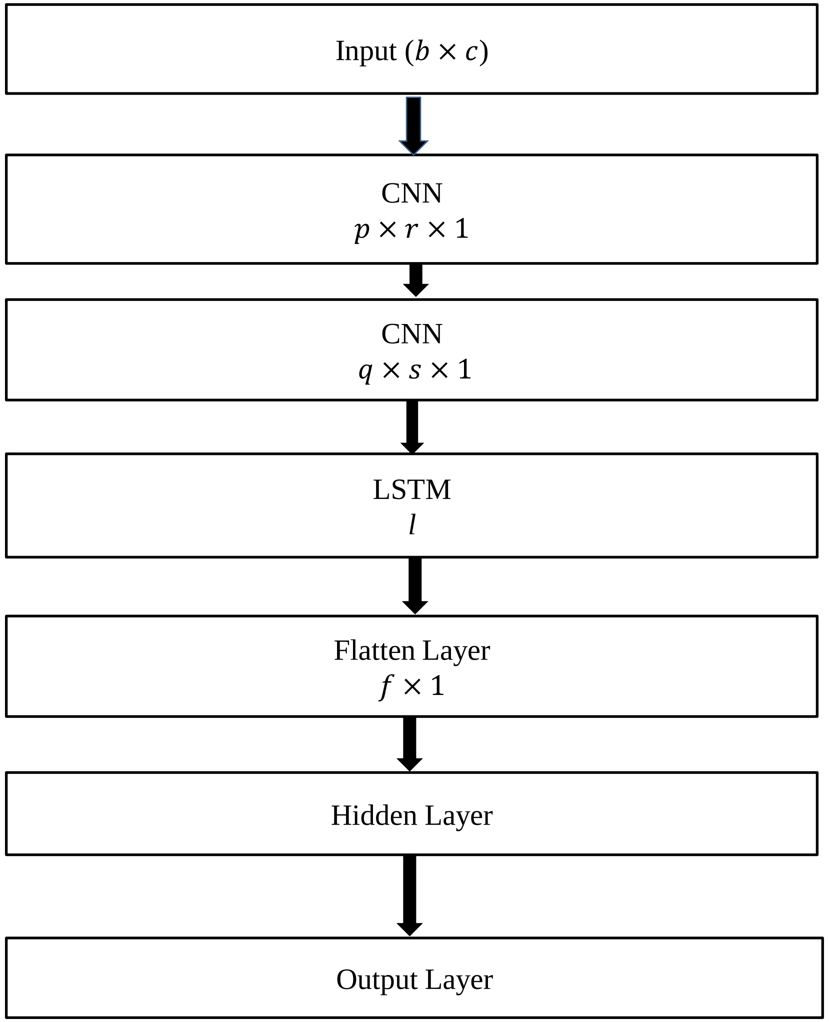

Figure. LRCN Topology.

Inertia Estimation Using GCN

- Power system is an interconnected network of generators and loads.
- The graph structure of the power system consists of nodes (buses) and edges (branches).
- Undirected graph represents power system

$$\mathcal{G} = (\mathcal{V}, \mathcal{E})$$

$$V = \widetilde{D}^{-\frac{1}{2}} \tilde{A} \widetilde{D}^{-\frac{1}{2}}$$

where $\tilde{A} = A + I_N$ represents an adjacency matrix with self-connections

$$A_{ij} = \begin{cases} 1;\ if\ \mathcal{V}_i, \mathcal{V}_j \in V, (\mathcal{V}_i, \mathcal{V}_j) \in E \\ 0;\ if\ \mathcal{V}_i, \mathcal{V}_j \in V, (\mathcal{V}_i, \mathcal{V}_j) \notin E \end{cases}$$

The diagonal degree matrix $\widetilde{D}$ for $\mathcal{G}$ is defined as $\widetilde{D}_{ii} = \sum_j \tilde{A}_{ij}$

Forward propagation equation of graph convolutional networks (GCN):

$$F^l(X, A) = \sigma\left(V F^{(l-1)}(X, A) W_k^l + b^l\right)$$

Results Analysis

Optimal Feature Combination Selection:

- Training dataset: 80%
- Validation dataset: 20%

- Optimal Combination: $\Delta\omega$ and $\Delta\dot{\omega}$

- Highest validation accuracy: 97.34% (tolerance 0.5s)

Table
Comparison of Different Features Sets for LRCN

Features Set	$\Delta\omega$	$\Delta\dot{\omega}$	$\Delta\omega$ + $\Delta\dot{\omega}$	$\Delta\omega$ + $\Delta\dot{\omega}$ + v
Validation Accuracy	80.30%	96.89%	97.34%	95.76%
MSE	0.296	0.032	0.025	0.030
Coefficient of Determination	0.8945	0.9585	0.9725	0.9564

Comparison of Models

- Combination of $\Delta\omega$ and $\Delta\dot{\omega}$
- GCN has the highest validation accuracy 98.15%

Table I
Comparison of Models with Optimal Feature Combination

Model	Validation Accuracy	Coefficient of Determination	MSE
DNN	93.45%	0.9224	0.058
CNN	95.18%	0.9369	0.045
LRCN	97.34%	0.9725	0.025
GCN	98.15%	0.9826	0.020

Signal to noise ratio (45dB)

- Combination of $\Delta\omega$, $\Delta\dot{\omega}$, and v
- GCN models: higher robustness

Table II Comparison of Models with SNR at 45dB

Model	w/o SNR	w/ SNR at 45dB
DNN	93.45%	90.84%
CNN	95.18%	92.13%
LRCN	97.34%	93.25%
GCN	98.15%	93.87%

Summary

- LRCN and GCN based learning algorithms are proposed to estimate system inertia constant
- The proposed LRCN model and GCN model also show high robustness under conditions with higher noises
- The approaches can also be applied to estimate inertia constant in realistic conditions

1. **Mingjian Tuo** and Xingpeng Li, "Long-term Recurrent Convolutional Networks-based Inertia Estimation using Ambient Measurements," in *2022 IEEE IAS Annual meeting, Oct. 2022.*
2. **Mingjian Tuo** and Xingpeng Li, "Machine Learning Assisted Inertia Estimation using Ambient Measurements," *IEEE Transactions on Industrial Applications, April. 2023.*

1. Introductions
2. Physics-based Inertia Estimation
3. Machine Learning Assisted Inertia Estimation
4. Physics-based Locational RoCoF-constrained Unit Commitment
5. Deep Learning based RCUC
6. Active Linearized Sparse Neural Network based FCUC
7. Conclusion and Future Work

Basic SCUC Model

- We consider a power network comprising of G generating units, N loads, K branches, N buses.
- Optimization Problem:

$$\min_{\Phi} \sum_{g \in G} \sum_{t \in T} \left(c_g P_{g,t} + c_g^{\mathrm{NL}} u_{g,t} + c_g^{\mathrm{SU}} v_{g,t} + c_g^{\mathrm{RE}} r_{g,t} \right) \quad (13a)$$

$$\sum_{g \in G} P_{g,t} + \sum_{k \in K(n-)} P_{g,t} - \sum_{k \in K(n+)} P_{g,t} - D_{n,t}$$

$$+ E_{n,t} = 0, \quad \forall n,\ t, \quad (13b)$$

$$P_{k,t} - b_k(\theta_{n,t} - \theta_{m,t}) = 0, \quad \forall k,\ t, \quad (13c)$$

$$-P_k^{\max} \le P_{k,t} \le P_k^{\max}, \quad \forall k,\ t, \quad (13d)$$

$$P_g^{\min} u_{g,t} \le P_{g,t}, \quad \forall g, t, \quad (13e)$$

$$P_{g,t} + r_{g,t} \le u_{g,t} P_g^{\max}, \quad \forall g, t, \quad (13f)$$

$$0 \le r_{g,t} \le R_g^{\mathrm{re}} u_{g,t}, \quad \forall g, t, \quad (13g)$$

$$\sum_{j \in G} r_{j,t} \ge P_{g,t} + r_{g,t}, \quad \forall g, t, \quad (13h)$$

$$P_{g,t} - P_{g,t-1} \le R_g^{\mathrm{hr}}, \quad \forall g, t, \quad (13i)$$

$$P_{g,t-1} - P_{g,t} \le R_g^{\mathrm{hr}}, \quad \forall g, t, \quad (13j)$$

$$v_{g,t} \ge u_{g,t} - u_{g,t-1}, \quad \forall g, t, \quad (13k)$$

$$v_{g,t+1} \le 1 - u_{g,t} \quad \forall g, t \le nT - 1, \quad (13l)$$

$$v_{g,t} \le u_{g,t} \quad \forall g, t, \quad (13m)$$

$$v_{g,t} \in \{0, 1\}, \quad \forall g, t, \quad (13n)$$

$$u_{g,t} \in \{0, 1\}, \quad \forall g, t, \quad (13o)$$

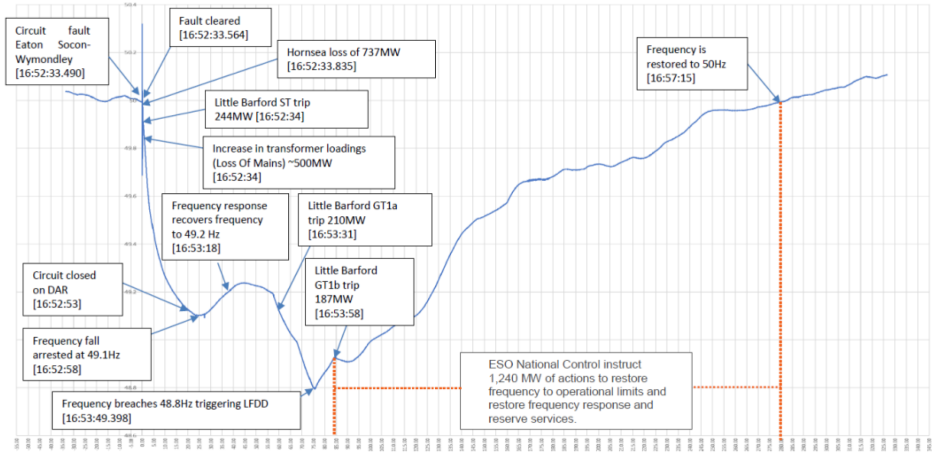

Figure. System frequency during the power disruption, August 2019

Additional frequency related constraints are needed

[Reference] **Mingjian Tuo** and Xingpeng Li, "Security-Constrained Unit Commitment Considering Locational Frequency Stability in Low-Inertia Power Grids" , *IEEE Transaction on Power System, Oct 2022*.

[Reference] August 2019 Power Disruption in Great Britain System Report.

System Dynamic Model

System Equivalent/Uniform Model (inaccurate)

$$M\frac{d \triangle \omega}{dt} + D \triangle \omega = P_m - P_e$$

The actual need for frequency ancillary services would be underestimated, leading to higher perceived nodal RoCoF.

Using the topological information and system parameters, the oscillatory behavior of each individual bus,

$$m_i\ddot{\theta}_i + d_i\dot{\theta}_i = p_{in,i} - p_{e,i} \qquad (1)$$

$$p_{e,i} = \sum_{j=1}^{n} b_{ij}(\theta_i - \theta_j),\ i \in \{1, \dots, n\} \qquad (2)$$

By combining (1) and (2) and eliminating passive load buses, a network-reduced model (Kron Reduction) with *N* generator buses.

$$M\ddot{\theta} + D\,\dot{\theta} = P - L\,\theta$$

where L is the Laplacian matrix of the reduced grid and it is real and symmetric.

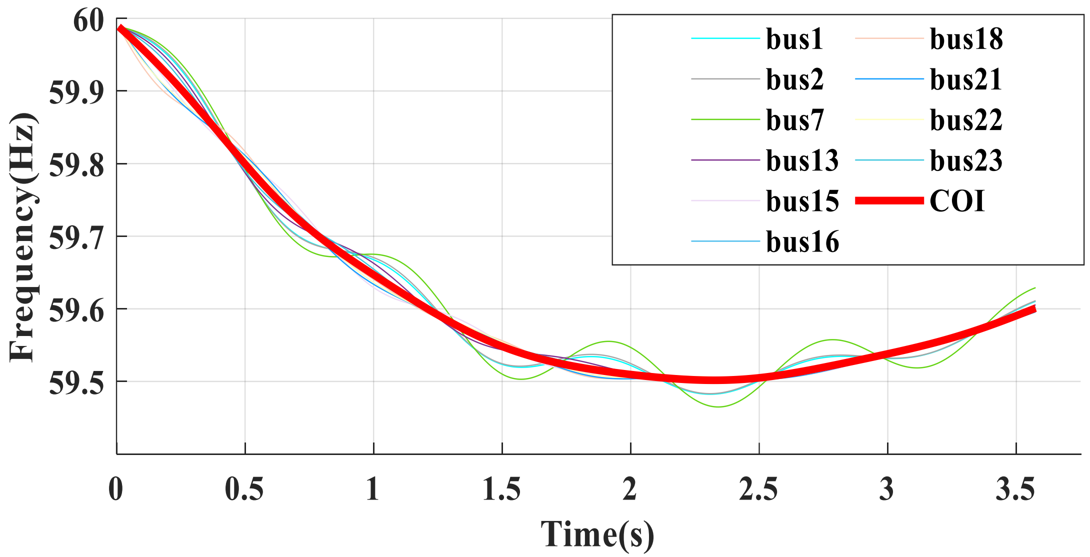

Figure. Frequency dynamics on generator buses in IEEE-24 bus system

Nodal RoCoF Expression

The RoCoF $R_i(t)$ on bus i can be calculated as:

$$R_i(t)=\frac{\Delta P e^{-\frac{\gamma t}{2}}}{2\pi m}\sum_{\alpha=1}^{N}\frac{\boldsymbol{\beta_{\alpha i}\beta_{\alpha b}}}{\sqrt{\frac{\lambda_\alpha}{m}-\frac{\gamma^2}{4}}\Delta t}\times\left[e^{-\frac{\gamma\Delta t}{2}}\sin\left(\sqrt{\frac{\lambda_\alpha}{m}-\frac{\gamma^2}{4}}(t+\Delta t)\right)-\sin\left(\sqrt{\frac{\lambda_\alpha}{m}-\frac{\gamma^2}{4}}t\right)\right]$$

- $\boldsymbol{\beta_{\alpha i}}$ is defined as Fiedler mode that affects the locational frequency dynamics.
- Higher oscillations occur on buses with large absolute value of Fiedler mode ($\boldsymbol{\beta_{\alpha i}}$).

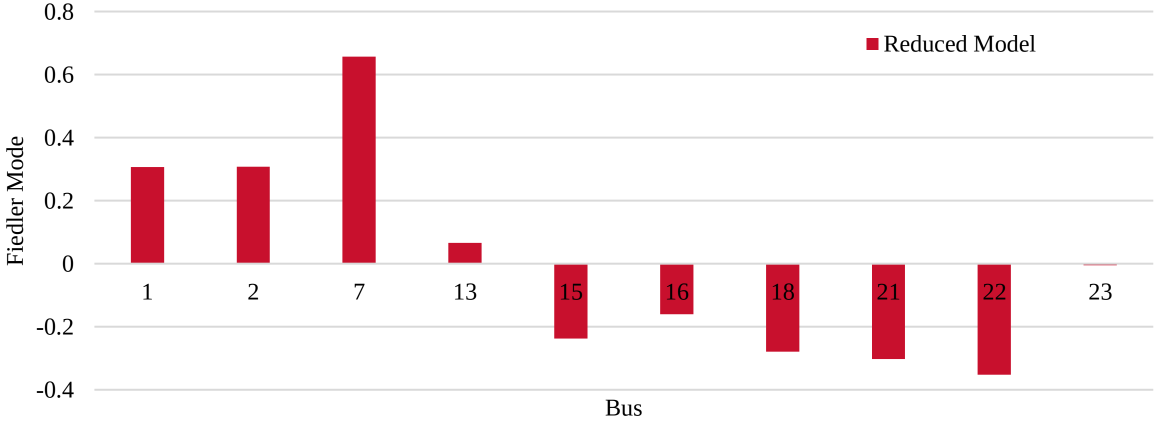

Fig. 1 Fiedler mode distribution

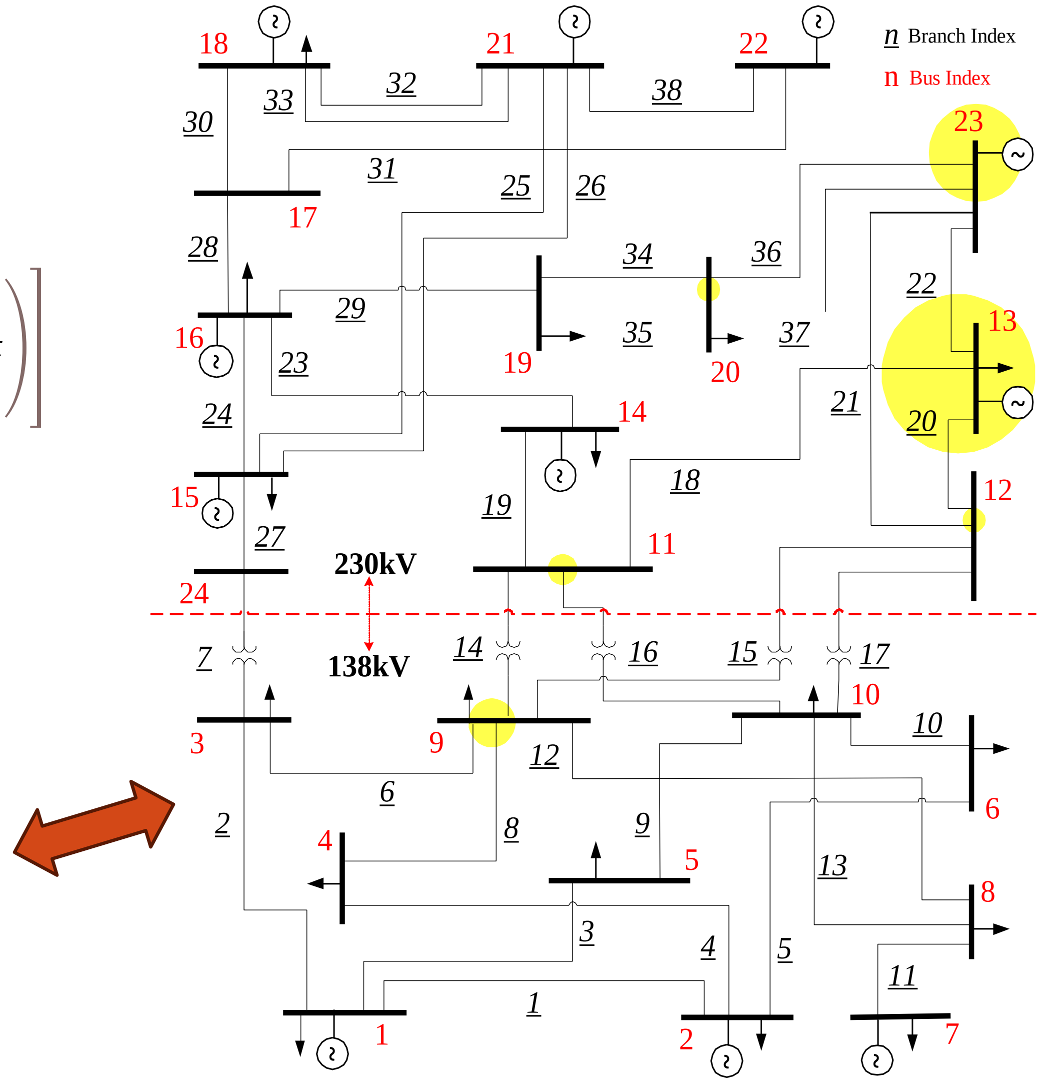

Fig.2 Center of inertia area estimation in IEEE 24-bus system.

Locational frequency constraints (LRC)

G-1 contingency of largest generation is considered as the **worst contingency** in this study.

- Mismatch in system power balance.
- Decreases the system synchronous inertia, resulting in higher frequency deviation and larger initial RoCoF.

- Then RoCoF constraints considering ΔP_{loss} can be defined as:

$$\frac{\Delta P_{loss} e^{-\gamma\frac{t}{2}}\left(1 - e^{-\gamma\Delta t}\right)}{2N\pi(m - \Delta m)\gamma\Delta t} + \frac{\Delta P_{loss} e^{-\gamma\frac{t}{2}}}{2\pi(m - \Delta m)} \times \frac{\boldsymbol{\beta_{2i}\beta_{2b}}}{\sqrt{\frac{\lambda_2}{m - \Delta m} - \frac{\gamma^2}{4}}\Delta t}$$

$$\left[e^{-\gamma\frac{\Delta t}{2}} \sin\left(\sqrt{\frac{\lambda_2}{m-\Delta m} - \frac{\gamma^2}{4}}(t + \Delta t)\right) - \sin\left(\sqrt{\frac{\lambda_2}{m-\Delta m} - \frac{\gamma^2}{4}}\, t\right)\right] \leq -RoCoF_{lim}\ (0.5\ \text{Hz/s})$$

LRC-SCUC Model

Objective function

$$min \sum_{g\in G}\sum_{t\in T}\left(c_g P_{gt} + c_g^{NL} u_{gt} + c_g^{SU} v_{gt} + c_g^{RE}\, r_{g,t}\right)$$

Additional constraints:

non-linear constraints

$$\underbrace{\frac{p_{g,t} e^{-\gamma\frac{t}{2}}\left(1-e^{-\gamma\Delta t}\right)}{2N m_{gt}\pi\gamma\Delta t} + \frac{p_{g,t} e^{-\gamma\frac{t}{2}}}{2\pi m_{gt} t}\frac{\beta_{2n}\beta_{2b}}{\sqrt{\frac{\lambda_2}{m_{gt}}-\frac{\gamma^2}{4}}\Delta t}\left[e^{-\gamma\frac{\Delta t}{2}}\sin\left(\sqrt{\frac{\lambda_2}{m_{gt}}-\frac{\gamma^2}{4}}(t+\Delta t)\right)-\sin\left(\sqrt{\frac{\lambda_2}{m_{gt}}-\frac{\gamma^2}{4}}\,t\right)\right]}_{\boldsymbol{f(x)}} \le -RoCoF_{lim}, \forall n \in N_{nl}, g\ , t$$

where m_{gt} is the average nodal inertia of in period t:

$$m_{gt} = \frac{\sum_{j\in G} 2H_j k_{j,t} - 2H_g k_{g,t}}{N\omega_0}\quad \forall g, t,$$

Piecewise Linearization

A least squares based piecewise linearization (PWL) technique is employed to formulate a RoCoF linearization problem.

$$\min_{\Psi} \sum_{\eta} \left(\max_{1 \le v \le q} \{w_v x + d_v\} - f(x) \right)^2$$

η denotes the evaluation point

Ψ denotes w_v, a_v for $1 \le v \le q$

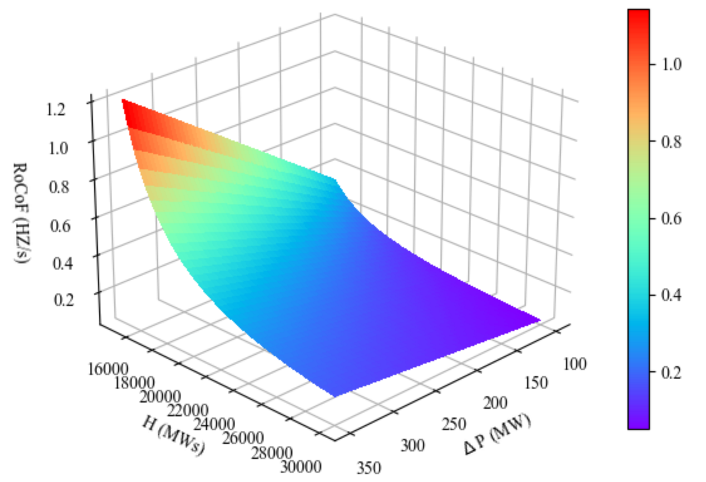

Figure. RoCoF of bus 21 following a *G*-1 contingency.

$$\min_{\Psi} \sum_{\eta} \left(t_q - f(x) \right)^2$$

$$\text{s.t.} \quad w_1 x + d_1 \le t_1 \le w_1 x + d_1 + \varepsilon_1 M \,, \forall \eta$$

$$w_2 x + d_2 \le t_1 \le w_2 x + d_2 + (1 - \varepsilon_1) M \,, \forall \eta$$

$$t_{v-1} \le t_v \le t_{v-1} + \varepsilon_2 M \,, \forall \eta, v \ge 2$$

$$w_{v+1} x + d_{v+1} \le t_v \le w_{v+1} x + d_{v+1} + (1 - \varepsilon_2) M \,, \forall \eta, v \ge 2$$

Define new ancillary variables:

$$t_1 = max\{ w_1 x + d_1, w_2 x + d_2 \}$$

$$t_v = max\{ t_{v-1}, w_{v+1} x + d_{v+1} \}, v \ge 2$$

SCUC Models Settings

Proposed model:

- location based RoCoF constrained SCUC (LRC-SCUC)

Benchmark models:

- Traditional SCUC (T-SCUC)
    - Does not consider any frequency related constraints.
- System equivalent model based RoCoF constrained SCUC (ERC-SCUC)
    - Consider system-wide frequency constraints
    - ignore the inter-area oscillations.

$$E_{sys} = \frac{-P_G}{2 \cdot RoCoF_{lim}} \cdot \omega_0 \geq E_{threshold}$$

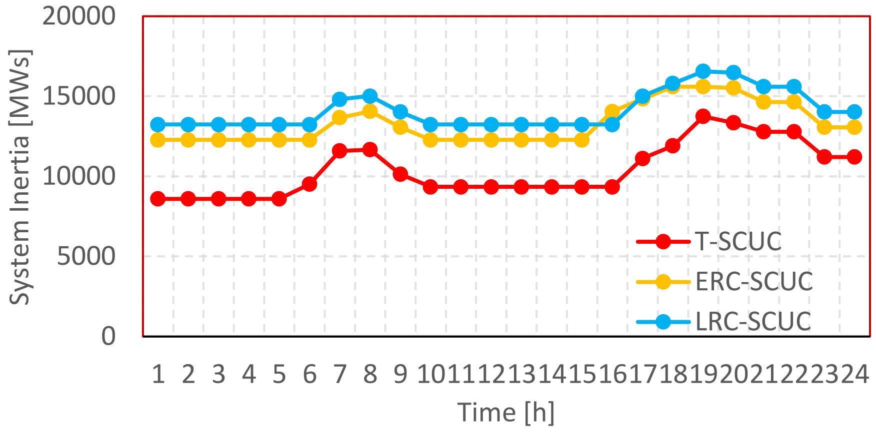

Fig. 1 Impact of RoCoF constraints on the total system inertia.

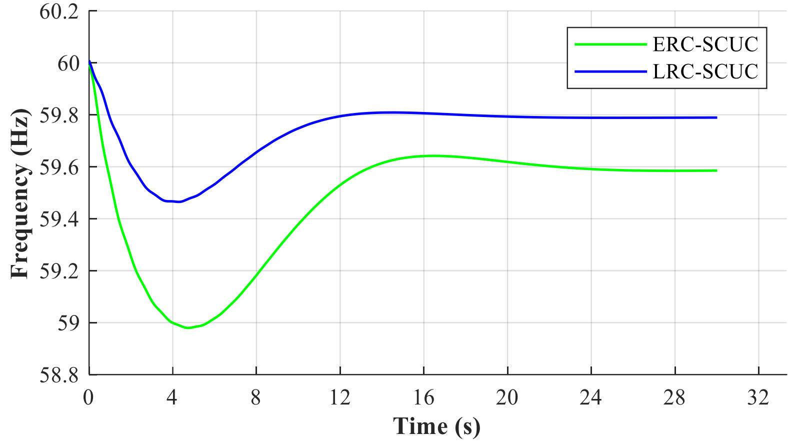

Fig. 2 System frequency response after loss of the generator with the largest generation.

Time Domain Simulation

- Transient Stability Analysis Tools (TSAT)
- ERC-SCUC and T-SCUC models:
  - The highest RoCoF violates the prescribed threshold (0.5 Hz/s).
  - Lower total cost in all scenarios.
- Proposed LRC-SCUC model:
  - The highest RoCoFs over all buses are all within the safe range.
  - Extra operational cost.
  - Low-cost virtual inertia services, the system total cost can be significantly reduced.

Table Highest RoCOF [Hz/s] monitored under different scenarios at peak hour

Model	RES Penetration Level			
	20%	40%	60%	80%
T-SCUC	1.26	1.32	1.45	1.65
ERC-SCUC	0.74	0.65	0.63	0.61
LRC-SCUC	0.34	0.38	0.42	0.46

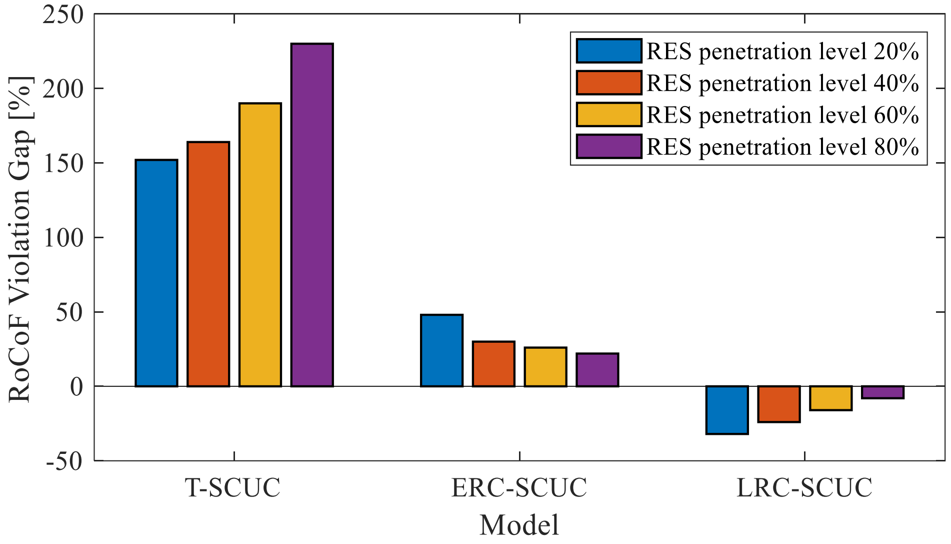

Figure. RoCoF violation gaps for different scenarios.

Inertial Response

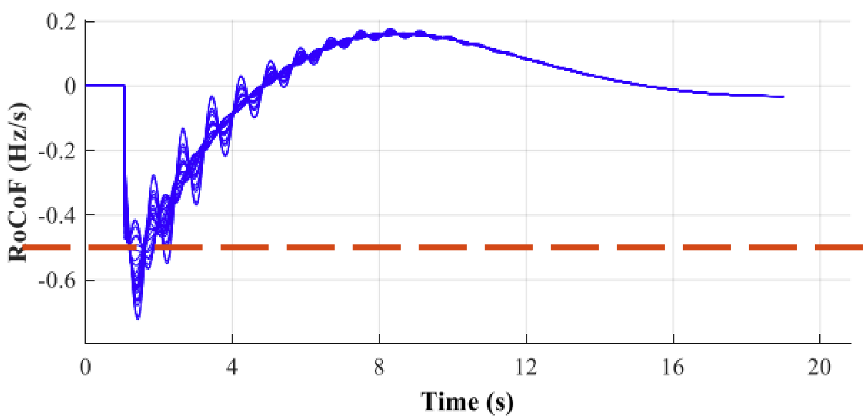

Fig. 1 RoCoF of all buses following the loss of largest generation in ERC-SCUC case.

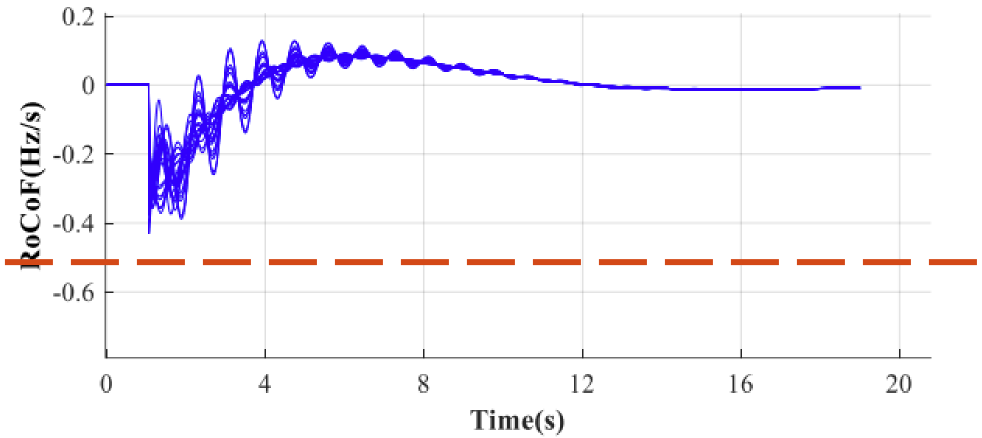

Fig. 2 RoCoF of all buses following the loss of largest generation in LRC-SCUC case.

- Benchmark ERC-SCUC: the highest locational RoCoF (0.7 Hz/s) violates the RoCoF security limit.
- Proposed LRC-SCUC: the highest locational RoCoF is 0.43 Hz/s, meeting the RoCoF security requirement.

Summary

- Locational RoCoF Constrained-SCUC (LRC-SCUC) is proposed in this chapter
  - Frequency dynamics model on reduced system are derived
  - RoCoF related constraints are proposed and incorporated into SCUC
  - RoCoF stability on all buses are secured. The impact of oscillations within the system is well handled

1. **Mingjian Tuo** and Xingpeng Li, "Optimal Allocation of Virtual Inertia Devices for Enhancing Frequency Stability in Low-Inertia Power Systems", *53rd North American Power Symposium (NAPS)*, Nov. 2021, College Station, TX, USA.
2. **Mingjian Tuo** and Xingpeng Li, "Security-Constrained Unit Commitment Considering Locational Frequency Stability in Low-Inertia Power Grids" , *IEEE Transactions on Power Systems, Oct 2022, Early Access Online* .

Mathematical Programing-based Scheduling

Conservative!

- ERC-SCUC model
- LRC-SCUC model

$$M\frac{d\bigtriangleup\omega}{dt}+D\bigtriangleup\omega=P_m-P_e$$

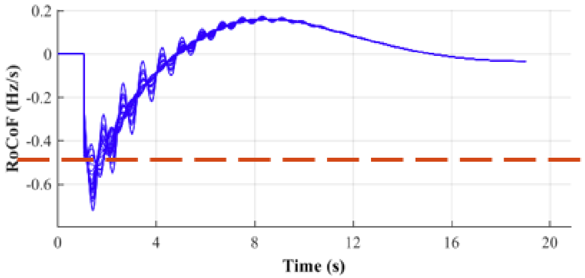

Fig. RoCoF of all buses following the loss of largest generation in ERC-SCUC case.

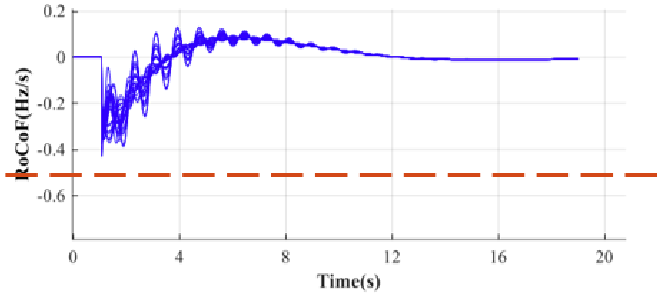

Fig. RoCoF of all buses following the loss of largest generation in LRC-SCUC case.

Dynamic validation, and update UC model iteratively!

Disadvantages of mathematical programming-based (MP-based) scheduling:

- Rely on the low-order model approximation that cannot be able to capture the entire characteristics
- These methods cannot incorporate high-order models. Nonlinearities in system frequency response such as deadbands, and saturations cannot be taken into considerations.

NN-based Scheduling

Additional constraints:

non-linear constraints

$$\underbrace{\begin{aligned}&\frac{p_{g,t}e^{-\gamma\frac{t}{2}}\left(1-e^{-\gamma\Delta t}\right)}{2Nm_{gt}\pi\gamma\Delta t}+\frac{p_{g,t}e^{-\gamma\frac{t}{2}}}{2\pi m_{gt}t}\frac{\beta_{2n}\beta_{2b}}{\sqrt{\frac{\lambda_2}{m_{gt}}-\frac{\gamma^2}{4}}\Delta t}\\&\left[e^{-\gamma\frac{\Delta t}{2}}\sin\left(\sqrt{\frac{\lambda_2}{m_{gt}}-\frac{\gamma^2}{4}}(t+\Delta t)\right)-\sin\left(\sqrt{\frac{\lambda_2}{m_{gt}}-\frac{\gamma^2}{4}}t\right)\right]\end{aligned}}_{\boldsymbol{f(x)}} \le RoCoF_{lim}, \forall n \in N_{nl}, g, t$$

Replace

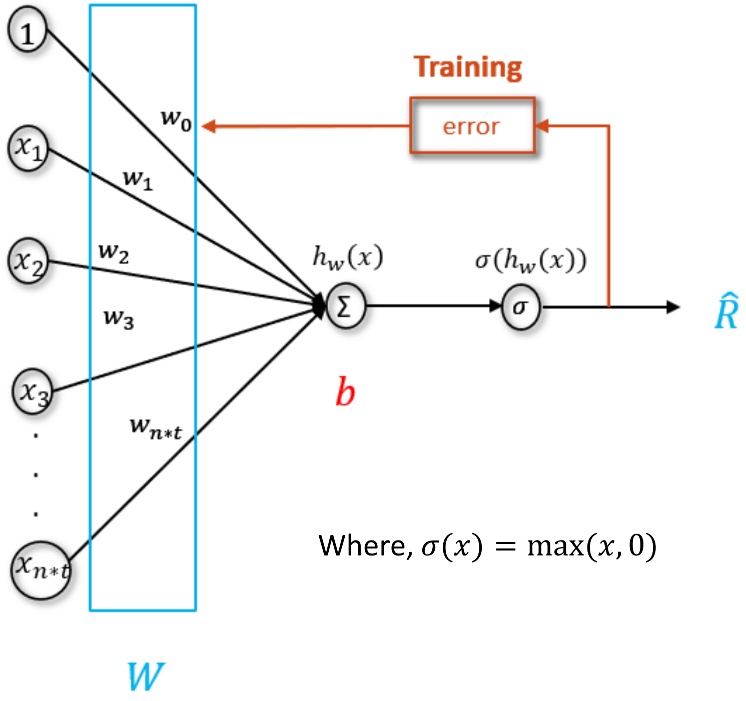

Where, $\sigma(x) = \max(x, 0)$

DNN has the ability to amend the limitations of MP-based approaches. The neural network based systemwide RoCoF predictor $\hat{h}$ can be expressed as:

$$\hat{R} = \hat{h}(x, W, b)$$

where *x* denotes the feature vector, and *W* and *b* denote the neural network parameters to be trained.

$$h_1 = x_1 W_1 + b_1$$

$$\hat{h}_m = h_{m-1} W_m + b_m$$

$$h_m = max(\hat{h}_m, 0)$$

$$\hat{R} = h_n W_n + b_n$$

[Reference] Arun Venkatesh Ramesh and Xingpeng Li, “Machine Learning Assisted Model Reduction for Security Constrained Unit Commitment”, *North American Power Symposium*, Salt Lake City, UT, USA, Oct. 2022.

Features Settings (DNN/CNN)

Input Features: $x_s = [u_s, \varpi_s^G, P_s]$

- The generator status feature vector u_s

$$u_s = [u_{1,s}, u_{2,s}, \cdots, u_{N_G,s}]$$

- The magnitude and location of the contingency ϖ_s^G

$$\varpi_s^G = \Big[0, \cdots, 0, \underbrace{P_s^{\varpi}}_{g_s^{\varpi} th\ element}, 0, \cdots, 0\Big]$$

$$P_s^{\varpi} = \max_{g \in G}(P_{1,s}, \cdots, P_{2,s}, \cdots, P_{N_G,s})$$

A big-M method is introduced to express the disturbance vector

- The active power injection of synchronous generator P_s.

New Input Features:

$$x_s = [u_{1,s}, \cdots, u_{N_G,s}, \varepsilon_{g,s}, \cdots, \varepsilon_{N_G,s}, P_{1,s}, \cdots, P_{N_G,s}]$$

$$z_1 = x_s W_1 + b_1$$

$$\hat{z}_q = z_{q-1} W_q + b_q$$

$$z_q = \max(\hat{z}_q, 0)$$

$$R_{h,s} = z_{N_L} W_{N_L+1} + b_{N_L+1}$$

$$\boldsymbol{ReLU(x) = max(x, 0)}$$

non-linear

Incorporation of NN model

NN-RCUC:

NN is incorporated into MILP problems by introducing auxiliary binary variables $a^{q}_{i,j,\epsilon.s}$.

$$z^{q}_{i,j,\epsilon,s} \leq \hat{z}^{q}_{i,j,\epsilon,s} + A(1 - a^{q}_{i,j,\epsilon,s}), \forall q, \forall \epsilon, \forall s, \forall i, \forall j,$$

$$z^{q}_{i,j,\epsilon,s} \geq \hat{z}^{q}_{i,j,\epsilon,s}, \forall q, \forall \epsilon, \forall s, \forall i, \forall j,$$

$$z^{q}_{i,j,\epsilon,s} \leq A a^{q}_{i,j,\epsilon,s}, \forall q, \forall \epsilon, \forall s, \forall i, \forall j,$$

$$z^{q}_{i,j,\epsilon,s} \geq 0, \forall q, \forall \epsilon, \forall s, \forall i, \forall j,$$

$$a^{q}_{i,j,\epsilon,s} \in \{0, 1\}, \forall q, \forall \epsilon, \forall s, \forall i, \forall j,$$

$$\boldsymbol{ReLU(x) = max(x, 0)}$$

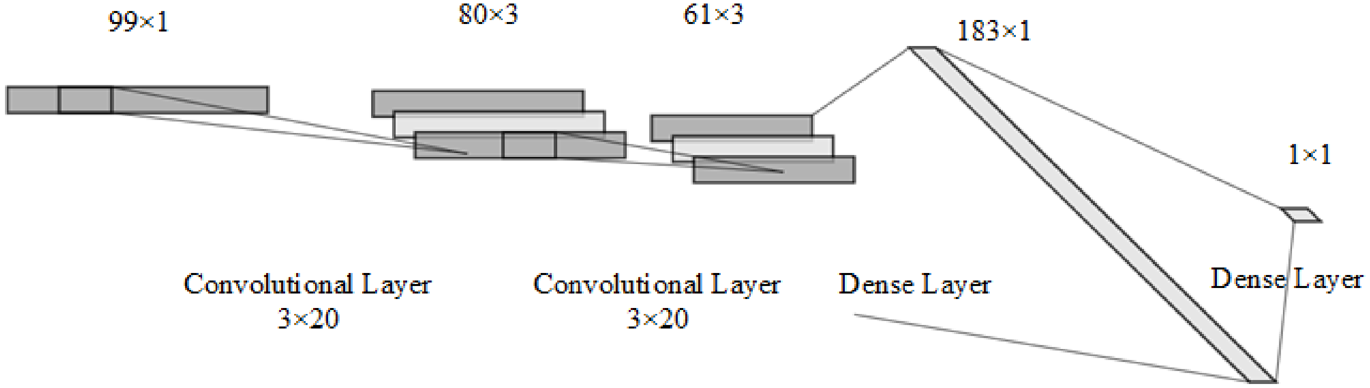

Figure. Architecture of proposed CNN model (Created using tool NN-SVG).

Test Case of DNN-RCUC

- IEEE 24-bus system (33 generators), PSS/E
- MP-based models:
  - Lower total cost.
  - Approximation error may result in violations
- DNN-RCUC model (4 periods constrained):
  - Maintain RoCoF within safe range following contingency of generator loss.
  - MP-based models cannot ensure system RoCoF security under same situation.
  - **Computational time increased**

Table Comparison of Different Models

Model	Total Cost [$]	Computational Time [s]	Highest RoCoF [Hz/s]
T-SCUC	1486556.34	13.58	0.8053
ERC-SCUC	1494430.99	20.24	0.6145
LRC-SCUC	1615135.45	35.25	0.5634
DNN-RCUC	1641966.76	$\boxed{368.58}$	$\boxed{0.4985}$

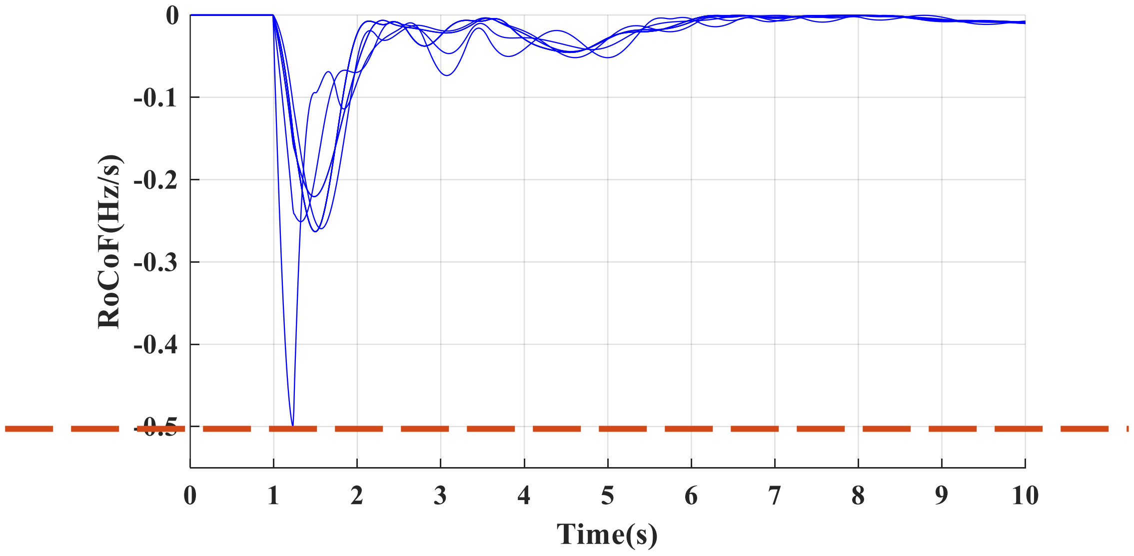

Figure. RoCoF evolution of DNN-RCUC model.

Test Case of CNN-RCUC

- CNN-RCUC model:
  - Maintain RoCoF within safe range following contingency of generator loss.
  - MP-based models cannot ensure system RoCoF security under same situation.

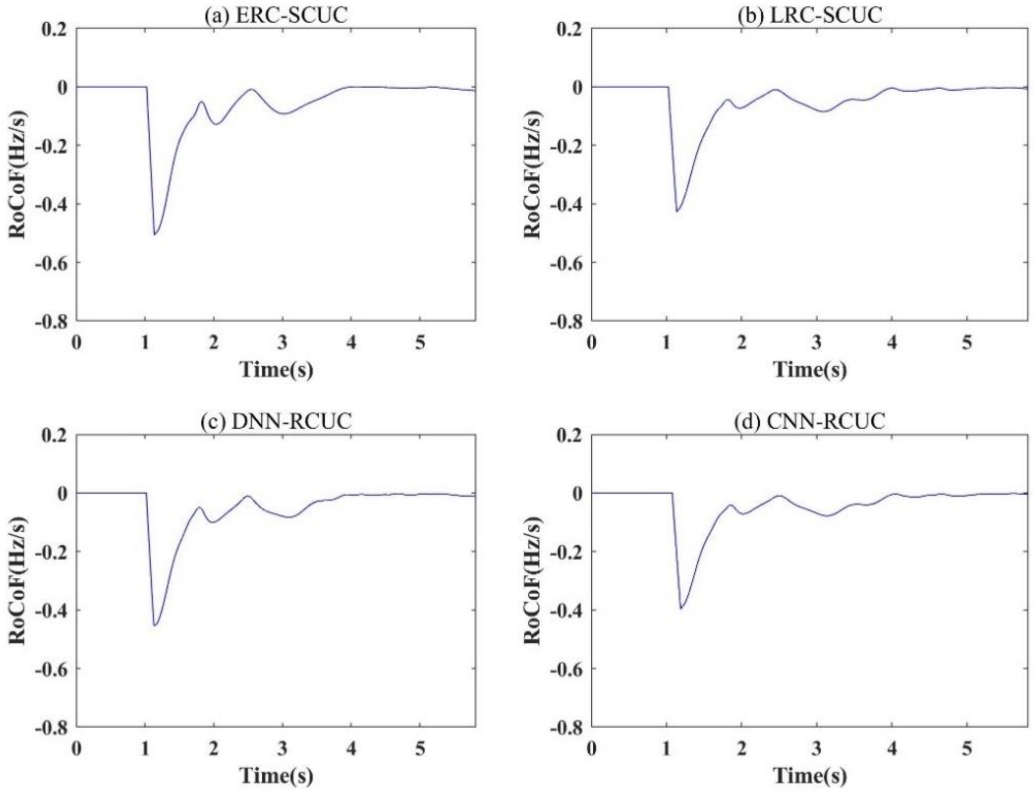

Fig. 1 Uniform RoCoF evolution of all cases.

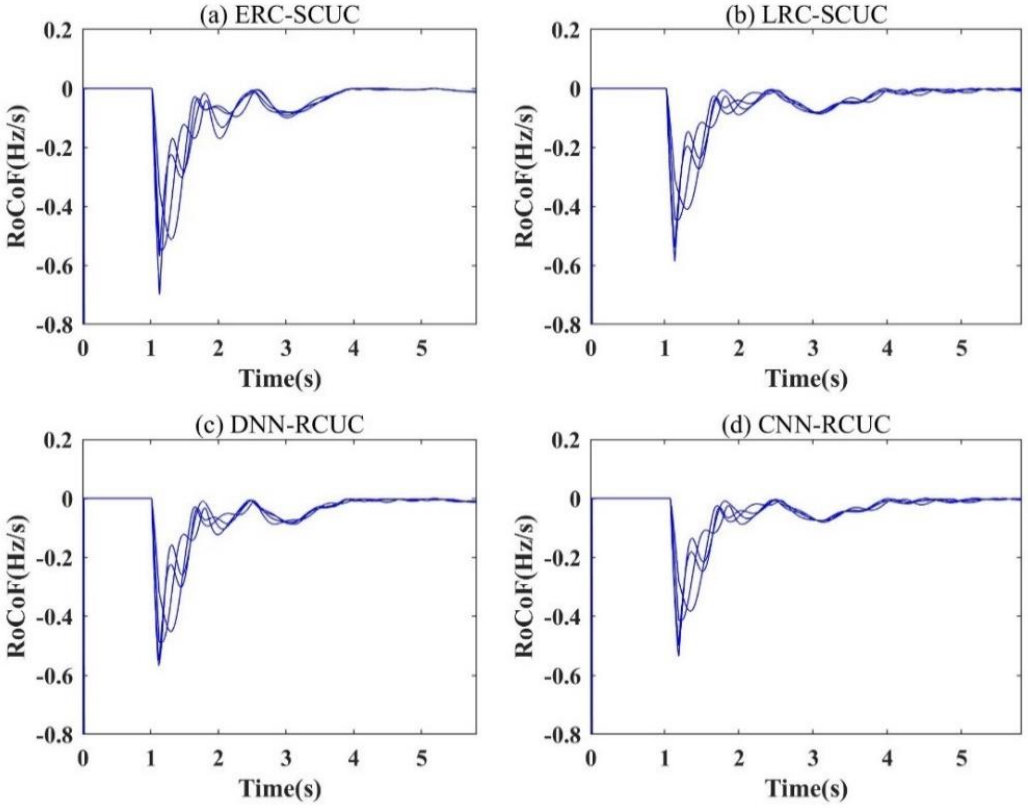

Fig. 2 Nodal RoCoF evolution of all cases.

Summary

- DNN/CNN-RCUC have better performance than physics-based approaches such as ERC-SCUC and LRC-SCUC

- Data-driven approaches maintain the RoCoF within safe range with less conservativeness (computational time increases).

- The proposed data generation method can avoid divergency during time domain simulation

1. **Mingjian Tuo** and Xingpeng Li, "Deep Learning based Security-Constrained Unit Commitment Considering Locational Frequency Stability in Low-Inertia Power Systems", *54th North American Power Symposium (NAPS)*, Oct. 2022, pp. 1-6.
2. **Mingjian Tuo** and Xingpeng Li, "Active ReLU Linearized Neural Network based Frequency-Constrained Unit Commitment in Low-Inertia Power Systems", *55th North American Power Symposium (NAPS).* (Submitted)
3. **Mingjian Tuo** and Xingpeng Li, "Convolutional Neural Network based Frequency-Constrained Unit Commitment in Low-Inertia Power Systems" , *Electric Power Systems Research (EPSR)*, 2023 . (In Preparation)

1. Introductions
2. Physics-based Inertia Estimation
3. Machine Learning Assisted Inertia Estimation
4. Physics-based Locational RoCoF-constrained Unit Commitment
5. Deep Learning Based RCUC
6. Active Linearized Sparse Neural Network based FCUC
7. Conclusion And Future Work

Frequency Metrics Constraints

Ordinary SCUC model:

$$\min. \quad \mathcal{C}(s_t, u_t)$$

$$s.t. \quad \mathcal{F}(s_t, u_t, d_t, r_t) = 0, \mathcal{G}(s_t, u_t, d_t, r_t) \le 0, \forall t$$

Formulation of stability related constraints:

$$\hat{h}^f(s_t, u_t, r_t, \varpi_t) \le \varepsilon$$

$$\begin{bmatrix} \hat{f}_{dev} \\ \hat{f}_{rcf} \end{bmatrix} = \hat{h}^f(x_t, W^f, b^f)$$

Multiple system stability metrics: RoCoF + Nadir + ...

- Forward propagation of NN

$$z_1 = x_t W_1 + b_1$$

$$\hat{z}_q = z_{q-1} W_q + b_q$$

$$z_q = \max(\hat{z}_q, 0)$$

$$\text{Multi-predictions} \begin{cases} \hat{f}_{dev} = z_{N_L} W_{N_L+1}^{dev} + b_{N_L+1}^{dev} \\ \hat{f}_{rcf} = z_{N_L} W_{N_L+1}^{rcf} + b_{N_L+1}^{rcf} \end{cases}$$

Dynamic Pruning

Efficiency:

The sparsity of the parameter matrix is increased from an initial sparsity value s_0 to a final sparsity value s_{final} over a span of μ pruning steps with pruning frequency Δe

$$s_e = s_{final} + (s_0 - s_{final})\left(1 - \frac{e - e_0}{\mu \Delta e}\right)^3$$

for $e \in \{e_0, e_0 + \Delta e, \dots, e_0 + \mu\Delta e\}$

Trade off:

Gradually increasing the sparsity of the network allows the network training steps to recover from pruning-induced loss in accuracy.

Algorithm 1 Sparse Neural Network Training

Input: Training Dataset $\Theta = \{(x_1, y_1), \dots, (x_n, y_n)\}$, $\theta = \{W, b\}$, Mask generator $Sp(\cdot)$, Final Sparsity s_{final}, Initial epoch e_0, Pruning frequency Δe, Pruning times Q, Total Training Epochs E, Batch size B

Output: optimal sparse W, b

$W \leftarrow W_0$ ▷ Initialize W with Pretrained W_0
$b \leftarrow b_0$ ▷ Initialize b with Pretrained b_0
for $e = 1, 2, \dots, E$ **do**
  if $e \neq e_0 + \mu\Delta e (\mu \in Q)$ **then**
    $h_1, \dots, h_B \leftarrow SNN(\Theta_B, \theta)$
    $\Delta_\theta \leftarrow BP(\Theta_B, h_1, \dots, h_B, \theta)$
    $\theta \leftarrow LearningRule(\Delta_\theta, \theta)$
  else
    $W \leftarrow W \odot Sp(s_0, s_{final}, \mu, e)$
    $h_1, \dots, h_B \leftarrow SNN(\Theta_B, \theta)$
    $\Delta_\theta \leftarrow BP(\Theta_B, h_1, \dots, h_B, \theta)$
    $\theta \leftarrow LearningRule(\Delta_\theta, \theta, Sp(s_0, s_{final}, \mu, e))$
  end if
end for
return θ

Active ReLU Linearization

Approximation of ReLU function reduces the number of introduced **binary variables**.

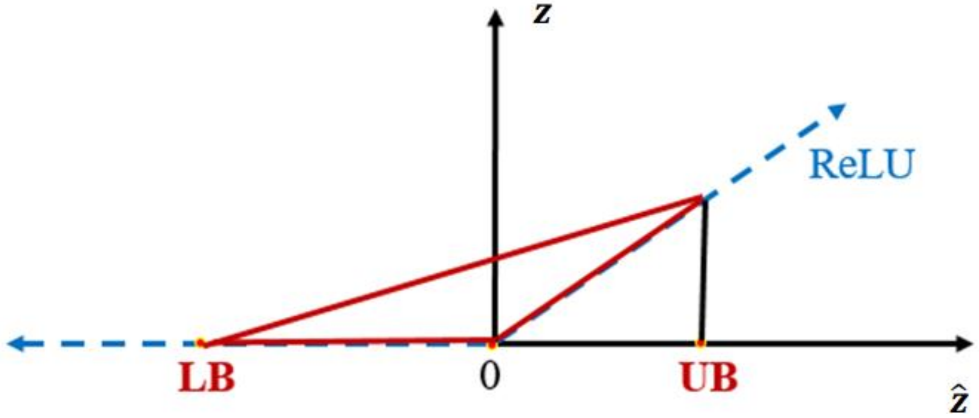

Linear equations replace mixed integer linear equations:

$$z_{q[l],s} \geq \hat{z}_{q[l],s}, \forall q, \forall l, \forall s,$$
$$z_{q[l],s} \leq \frac{UB_{q[l]} \cdot (\hat{z}_{q[l],s} - LB_{q[l]})}{UB_{q[l]} - LB_{q[l]}}, \forall q, \forall l, \forall s,$$
$$z_{q[l],s} \geq 0, \forall q, \forall l, \forall s,$$

Large approximation error and low prediction accuracy

- Active ReLU Linearization (partially linearized)
- Nodal positivity index

$$\varepsilon_{q[l]} = \frac{1}{N_S}\left(\sum_{N_S} \hat{z}_{q[l],s} - \sum_{N_S}\left|\hat{z}_{q[l],s} - \frac{1}{N_S}\sum_{N_S}\hat{z}_{q[l],s}\right|\right) \geq \delta$$

The neuron of each layer with positivity index $\varepsilon_{q[l]}$ larger than γ is selected out and added into set $\mathcal{H}$

$$z_1 = \boldsymbol{x}_t W_1 + b_1, \forall t,$$
$$z_{q[l],t} \geq \hat{z}_{q[l],t}, \forall q, \forall l \in \mathcal{H}, \forall t,$$
$$z_{q[l],t} \leq \frac{UB_{q[l]} \cdot (\hat{z}_{q[l],t} - LB_{q[l]})}{UB_{q[l]} - LB_{q[l]}}, \forall q, \forall l \in \mathcal{H}, \forall t,$$

ALSNN-FCUC Formulations

Active Linearized Sparse Neural Network based FCUC

Basic Formulations:

$$\min_{\Phi} \sum_{g\in G}\sum_{t\in T}(c_g P_{g,t} + c_g^{NL} u_{g,t} + c_g^{SU} v_{g,t} + c_g^{RE}\, r_{g,t})$$

$$\sum_{g\in G} P_{g,t} + \sum_{k\in K(n-)} P_{g,t} - \sum_{k\in K(n+)} P_{g,t} - D_{n,t} + E_{n,t} = 0, \quad \forall n,t$$

$$P_{k,t} - b_k(\theta_{n,t} - \theta_{m,t}) = 0, \quad \forall k,t$$

$$-P_k^{max} \leq P_{k,t} \leq P_k^{max}, \quad \forall k,t$$

$$P_g^{min} u_{g,t} \leq P_{g,t}, \quad \forall g,t$$

$$P_{g,t} + r_{g,t} \leq u_{g,t} P_g^{max}, \quad \forall g,t$$

$$0 \leq r_{g,t} \leq R_g^{re} u_{g,t}, \quad \forall g,t$$

$$\sum_{j\in G} r_{j,t} \geq P_{g,t} + r_{g,t}, \quad \forall g,t$$

…

Frequency related constraints (NN):

$$z_1 = \boldsymbol{x}_t W_1 + b_1, \forall t,$$

$$z_{q[l],t} \geq \hat{z}_{q[l],t}, \forall q, \forall l \in \mathcal{H}, \forall t,$$

$$z_{q[l],t} \leq \frac{UB_{q[l]} \cdot (\hat{z}_{q[l],t} - LB_{q[l]})}{UB_{q[l]} - LB_{q[l]}}, \forall q, \forall l \in \mathcal{H}, \forall t,$$

$$z_{q[l],t} \leq \hat{z}_{q[l],t} - A(1 - a_{q[l],t}), \forall q, l \in \bar{\mathcal{H}}, t,$$

$$z_{q[l],t} \geq \hat{z}_{q[l],t}, \forall q, \forall l \in \bar{\mathcal{H}}, \forall t,$$

$$z_{q[l],t} \leq A a_{q[l],t}, \forall q, \forall l \in \bar{\mathcal{H}}, \forall t,$$

$$z_{q[l],t} \geq 0, \forall q, \forall l, \forall t,$$

$$a_{q[l],t} \in \{0,1\}, \forall q, \forall l, \forall t,$$

$$z_{N_L,t} W_{N_L+1}^{dev} + b_{N_L+1}^{dev} \leq f_{nom} - f_{lim}$$

$$z_{N_L,t} W_{N_L+1}^{rcf} + b_{N_L+1}^{rcf} \leq -RoCoF_{lim}$$

Results Analysis

Settings (PSSE 35.0):

- GENROU and GENTPJ for the synchronous machine;
- IEEEX1 for the excitation system;
- IEESGO for the turbine-governor;
- PSS2A for the power system stabilizer.
- Standard WTG and corresponding control modules are employed.

The FCUC is performed using Pyomo and Gurobi on a window laptop with Intel(R) Core(TM) i7 2.60GHz CPU and 16 GB RAM.

- The predictor trained by active sampled dataset has higher robustness against sparsity

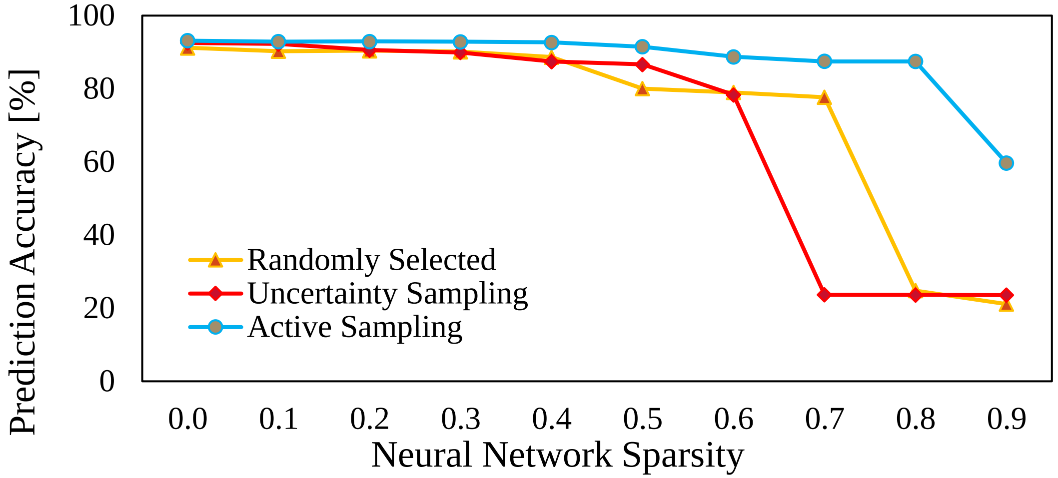

Fig. 1 RoCoF prediction accuracy with different NN sparsity.

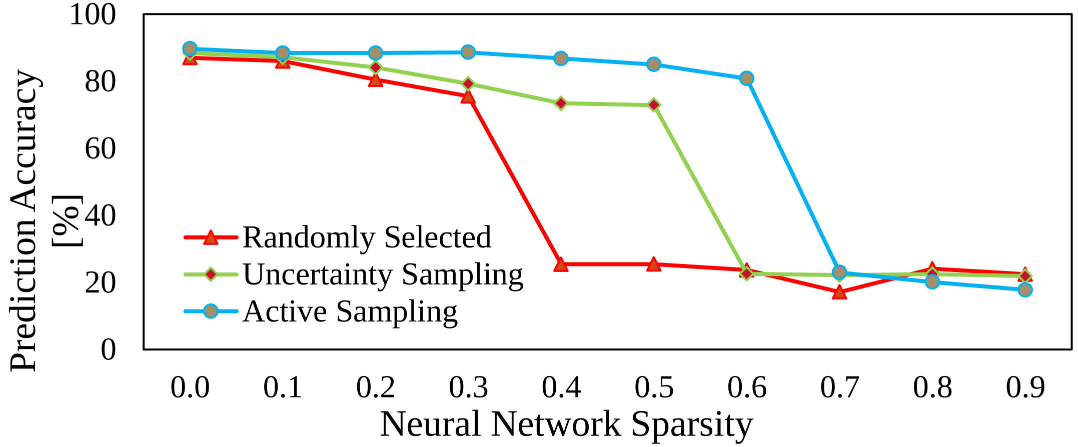

Fig. 2 Frequency deviation prediction accuracy with different NN sparsity.

Computational Time of MILP Model

Constraints bindingness (hour 10 constrained)

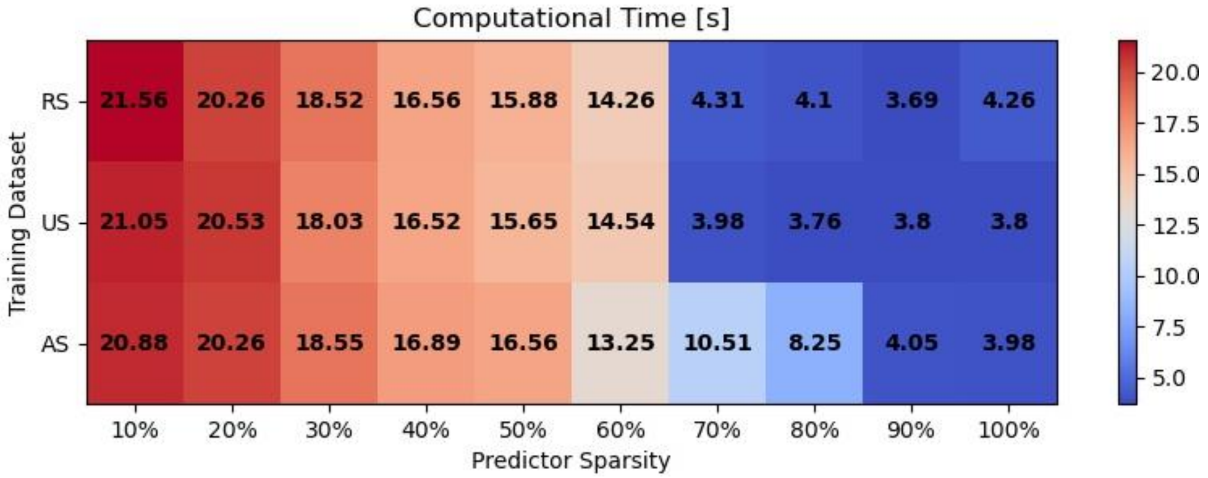

- Highest sparsity could lead to no-binding constraints and lowest computational time.
- Proposed active sampled dataset has higher robustness against sparsity.

Table Computational Time [s] of Different Constrained Intervals

Total Number of Constrained Hour	4	8	12	16	20	24
DNN-RCUC	23	268	523	NA	NA	NA
ALSNN-FCUC	8	14	50	143	254	1223

Time Limit: 7200 s

Without sparse computation and active linearization process, computational time increases exponentially.

Time Domain Simulation

- High sparsity could lead to no-binding constraints
- Active sampled dataset has higher robustness against sparsity (60%)

The proposed ALSNN-FCUC model can secure frequency stability with high efficiency

Table
Comparison of Different Models (hour 10 constrained)

Model	Total Cost [$]	Computational Time [s]	$\dot{f}_{max}$ [Hz/s]	Δf_{max} [Hz]
T-SCUC	419,935	3.89	1.05	0.51
ERC-SCUC	420,171	4.53	0.60	0.29
LRC-SCUC	425,929	6.05	0.44	0.23
DNN-FCUC	422,497	22.56	0.50	0.24
SNN-FCUC	421,922	16.56	0.50	0.23
ALSNN-FCUC	421,985	8.56	0.50	0.24

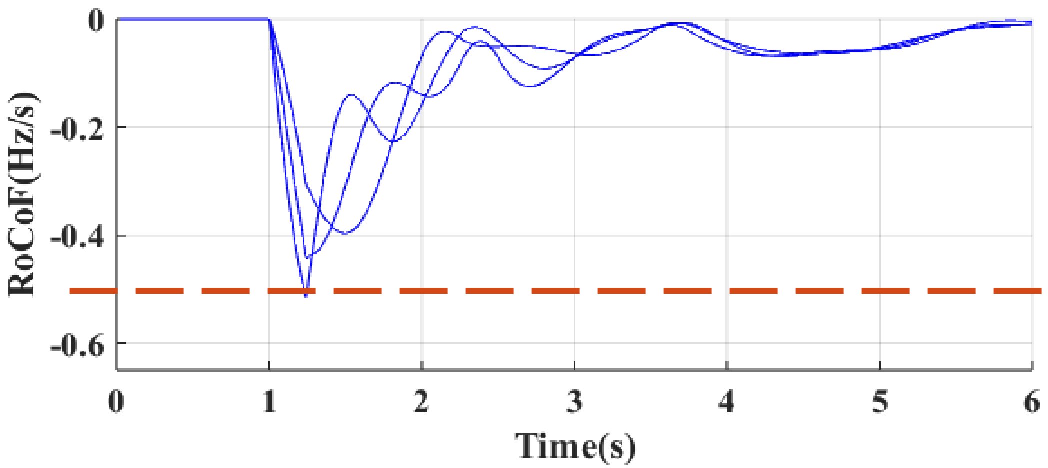

Figure. RoCoF evolution of ALSNN-FCUC model under worst contingency at hour 10.

Summary

- The proposed ALSNN-FCUC approach incorporates sparse computations to perform parameter selection.
- An active ReLU linearization method is performed over selected neurons to further improve the model efficiency.
- Results show that the model can maintain the system frequency related constraints under worst contingency while reducing the computational time

1. **Mingjian Tuo** and Xingpeng Li, "Sparsity Neural Network based Frequency-Constrained Unit Commitment with Region-of-Interest Active Sampling," *IEEE Transactions on Power Systems,* (Under review).

1. Introductions
2. Physics-based Inertia Estimation
3. Machine Learning Assisted Inertia Estimation
4. Physics-based Locational RoCoF-constrained Unit Commitment
5. Deep Learning based RCUC
6. Active Linearized Sparse Neural Network based FCUC
7. Conclusion and Future Work

Conclusions

- Current inertia estimation methods are limited by the accuracy of the measurements and the relative location of disturbance.
- Inertia distribution index is used as metric for inertia distribution analysis. Dynamic inertia estimation method based on COI area is proposed.
- Data driven inertia estimation approaches using wide area measurements, robustness of the proposed model has been tested under noisy condition.
- Equivalent/Uniform model cannot capture nodal characteristics. Dynamics model based on reduced system is proposed, nodal RoCoF expressions and related constraints are derived.
- LRC-SCUC model has been formulated. The highest RoCoFs over all buses are contained within the safe range, however the conservativeness issues are observed.
- DNN-RCUC/CNN-RCUC are introduced to maintain RoCoF within safe range with much less conservativeness (efficiency issues).
- ALSNN-FCUC model incorporates sparse computations to perform parameter selection and increase neural network sparsity, while securing frequency stability.

Future Work

- Implemented of GNN based method to relieve some constraints such as line congestions/generator status for efficiency for NN-SCUC.
- Variable reduction of SCUC could be implemented by predicting generator status and line loading factor using machine learning algorithms.
- Incorporation of inverter-based sources such as virtual machine and demand side synchronous motors.
- Proposed work can handle other dynamic performance such as voltage, steady state frequency.
- Data related weather patterns and scenarios can be studied.

Publications

1. **Mingjian Tuo**, Arun Venkatesh Ramesh and Xingpeng Li, "Benefits and Cyber-Vulnerability of Demand Response System in Real-Time Grid Operations," in *2020 IEEE International Conference on Communications, Control, and Computing Technologies for Smart Grids (SmartGridComm)*, Oct. 2020, pp. 1-6.
2. **Mingjian Tuo** and Xingpeng Li, "Dynamic Estimation of Power System Inertia Distribution Using Synchrophasor Measurements", in *52nd North American Power Symposium (NAPS)*, Apr. 2021, pp. 1-6, doi: 10.1109/NAPS50074.2021.9449713.
3. **Mingjian Tuo** and Xingpeng Li, "Long-term Recurrent Convolutional Networks-based Inertia Estimation using Ambient Measurements," in *2022 IEEE IAS Annual meeting, Oct. 2022.*
4. **Mingjian Tuo** and Xingpeng Li, "Optimal Allocation of Virtual Inertia Devices for Enhancing Frequency Stability in Low-Inertia Power Systems," in *53rd North American Power Symposium (NAPS)*, Nov. 2021, College Station, TX, USA.
5. **Mingjian Tuo** and Xingpeng Li, "Security-Constrained Unit Commitment Considering Locational Frequency Stability in Low-Inertia Power Grids" , *IEEE Transactions on Power Systems, Oct. 2022 (Early Access)*.
6. **Mingjian Tuo** and Xingpeng Li, "Deep Learning based Security-Constrained Unit Commitment Considering Locational Frequency Stability in Low-Inertia Power Systems," in *54th North American Power Symposium (NAPS)*, Oct. 2022, pp. 1-6.
7. Vasudharini Sridharan, **Mingjian Tuo**, Xingpeng Li, " Wholesale Electricity Price Forecasting using Integrated Long-term Recurrent Convolutional Network Model", *Energies, 2022*.
8. **Mingjian Tuo** and Xingpeng Li, "Active ReLU Linearized Neural Network based Frequency-Constrained Unit Commitment in Low-Inertia Power Systems" , in *55th North American Power Symposium (NAPS)*, 2023 (*Under Review*).
9. **Mingjian Tuo** and Xingpeng Li, "Machine Learning Assisted Inertia Estimation using Ambient Measurements," *IEEE Transactions on Industrial Applications. April. 2023. (Early Access).*
10. **Mingjian Tuo** and Xingpeng Li, "Sparsity Neural Network based Frequency-Constrained Unit Commitment with Region-of-Interest Active Sampling," *IEEE Transactions on Power Systems. (Under Review)*
11. **Mingjian Tuo** and Xingpeng Li, "Convolutional Neural Network based Security-Constrained Unit Commitment Considering Locational Frequency Stability in Low-Inertia Power Systems", *Electric Power Systems Research (EPSR)*, 2023 (In preparation)
12. **Mingjian Tuo** and Xingpeng Li, "Graph Neural Network based Power Flow Model", in *55th North American Power Symposium (NAPS)*, 2023 (*Under Review*)

UH RPG Lab

Thank you!

Mingjian Tuo
Cullen College of Engineering
University of Houston